Development/Plasticity/Repair

Mutually Repulsive EphA7–EfnA5 Organize Region-to-Region Corticopontine Projection by Inhibiting Collateral Extension

Tokuichi Iguchi,[1,2,3] Yuichiro Oka,[1,2,4] Misato Yasumura,[1] Minoru Omi,[2] Kazuki Kuroda,[2] Hideshi Yagi,[2] Min-Jue Xie,[2,4] Manabu Taniguchi,[1] Martin Bastmeyer,[5] and Makoto Sato[1,2,4,6,7]

[1]Department of Anatomy and Neuroscience, Graduate School of Medicine, Osaka University, Osaka 565-0871, Japan, [2]Division of Cell Biology and Neuroscience, Department of Morphological and Physiological Sciences, Faculty of Medical Sciences, University of Fukui, Fukui 910-1193, Japan, [3]Department of Nursing, Faculty of Health Science, Fukui Health Science University, Fukui 910-3190, Japan, [4]United Graduate School of Child Development, Osaka University, Kanazawa University, Hamamatsu University School of Medicine, Chiba University, and University of Fukui (UGSCD), Osaka University, Osaka 565-0871, Japan, [5]Department of Cell and Neurobiology, Zoological Institute, Karlsruhe Institute of Technology (KIT), 76131 Karlsruhe, Germany, [6]Graduate School of Frontier Biosciences, Osaka University, Osaka 565-0871, Japan, and [7]Research Center for Child Mental Development, University of Fukui, Fukui 910-1193, Japan

Coordination of skilled movements and motor planning relies on the formation of regionally restricted brain circuits that connect cortex with subcortical areas during embryonic development. Layer 5 neurons that are distributed across most cortical areas innervate the pontine nuclei (basilar pons) by protrusion and extension of collateral branches interstitially along their corticospinal extending axons. Pons-derived chemotropic cues are known to attract extending axons, but molecules that regulate collateral extension to create regionally segregated targeting patterns have not been identified. Here, we discovered that *EphA7* and *EfnA5* are expressed in the cortex and the basilar pons in a region-specific and mutually exclusive manner, and that their repulsive activities are essential for segregating collateral extensions from corticospinal axonal tracts in mice. Specifically, *EphA7* and *EfnA5* forward and reverse inhibitory signals direct collateral extension such that *EphA7*-positive frontal and occipital cortical areas extend their axon collaterals into the *EfnA5*-negative rostral part of the basilar pons, whereas *EfnA5*-positive parietal cortical areas extend their collaterals into the *EphA7*-negative caudal part of the basilar pons. Together, our results provide a molecular basis that explains how the corticopontine projection connects multimodal cortical outputs to their subcortical targets.

Key words: collateral; cortex; corticospinal tract; neuronal circuit; pontine nucleus

Significance Statement

Our findings put forward a model in which region-to-region connections between cortex and subcortical areas are shaped by mutually exclusive molecules to ensure the fidelity of regionally restricted circuitry. This model is distinct from earlier work showing that neuronal circuits within individual cortical modalities form in a topographical manner controlled by a gradient of axon guidance molecules. The principle that a shared molecular program of mutually repulsive signaling instructs regional organization—both within each brain region and between connected brain regions—may well be applicable to other contexts in which information is sorted by converging and diverging neuronal circuits.

Received Feb. 14, 2020; revised Mar. 31, 2021; accepted Apr. 14, 2021.

Author contributions: T.I. and M.S. designed research; T.I., Y.O., M.Y., M.O., and M.T. performed research; T.I., Y.O., M.Y., M.O., and M.S. analyzed data; K.K., H.Y., M.-J.X., and M.B. contributed unpublished reagents/analytic tools; T.I. and M.S. wrote the paper.

This work was supported in part by a Grant-in-Aid for Young Scientists (B) [Japan Society for the Promotion of Science (JSPS) KAKENHI 24700323 to T.I.], a Grant-in-Aid for Scientific Research (C) (JSPS KAKENHI 26430017 to T.I., JSPS KAKENHI 26430036 to MO, JSPS KAKENHI 19K06923 to M.Y.), Grant-in-Aid for Scientific Research (B) (JSPS KAKENHI 21390052, 25293043, and 17H04014 to M.S.), and Challenging Research (Exploratory) (JSPS KAKENHI 19K22471 to M.S.) from the Japan Society for the Promotion of Science. This study was supported by Center for Medical Research and Education (CentMeRE), Graduate School of Medicine, Osaka University; and by Life Science Research Laboratory, University of Fukui. We thank Non Profit Organization (NPO) Biotechnology Research and Development for technical assistance to generate EphA7$^{-/-}$ mouse; Y. Konishi and Y. Mori for helpful discussion and technical advice; H. Yoshikawa, S. Kanae, I. Kumano, H. Miyagoshi, A. Emi, and K. Kurose for technical assistance; T. Taniguchi, M. Yamaguchi, Y. Shibuya, and A. Yoshinori for secretarial assistance, F. Weth for critical reading; and C. Lilliehook for manuscript editing. We also thank J. Miyazaki for the pCAGGS vector. and H. Sakano and H. Takeuchi for the EfnA5-AP vector.

M. Omi's present address: Department of Anatomy I, Fujita Health University School of Medicine, Toyoake 470-1192, Aichi, Japan.

K. Kuroda's present address: Division of Brain Structure and Function, Department of Morphological and Physiological Sciences, Faculty of Medical Sciences, University of Fukui, Fukui 910-1193, Japan.

H. Yagi's present address: Department of Cell Biology, Hyogo College of Medicine, Nishinomiya 663-8501, Hyogo, Japan.

The authors declare no competing financial interests.

Correspondence should be addressed to Makoto Sato at makosato@anat2.med.osaka-u.ac.jp.

https://doi.org/10.1523/JNEUROSCI.0367-20.2021

Introduction

The neocortex acquires distinct areal identities during development and connects to target regions in a way that maintains the properties of their functional modality, such as motor, somatosensory, or visual information (O'Leary and Koester, 1993). Regional arrangement is critical to enable both efficient circuit formation during development and coordinated information processing in the adult. Subcortical projections from pyramidal neurons in cortical layer 5, which are the main output circuits from the neocortex, make regionally organized circuit connections to different subcortical brain areas (Greig et al., 2013). The mechanisms by which projections between cortical and subcortical areas develop to achieve this regional separation are poorly understood.

Among the subcortical targets of the neocortex, the pontine nucleus mediates information from the neocortex to the cerebellum, which in itself is not linked directly with cortex (Brodal and Bjaalie, 1992; Ramnani, 2006). The cerebellum develops the most in humans after birth, enabling us to achieve higher brain function such as cognitive processing and motor planning in addition to the coordination of skilled movements (Ramnani, 2006; Brissenden et al., 2018; Gao et al., 2018; Wagner and Luo, 2020). The corticopontine projection is a major subcortical projection, established by interstitial axon collaterals from axons arising from layer 5 neurons distributed across most areas of the neocortex. Several lines of studies indicate that pons-derived chemotropic cues are involved in the formation of this projection (Heffner et al., 1990; Sato et al., 1994; Zhu et al., 2009; Di Meglio et al., 2013), but a more detailed understanding of its developmental formation is lacking.

In adult rats, tracer studies show that corticopontine projections from most cerebral regions typically consist of several delineated clusters of fibers that distribute to segregated locations in the pontine nuclei to make regionally organized connections (Leergaard and Bjaalie, 2007; Leergaard et al., 1995). Importantly, in somatosensory and motor area of the neocortex, the corticopontine projections are collateral projections of corticospinal tract of the same layer 5 neurons. In other areas, such as the visual cortex, corticopontine neurons form projections to the spinal cord during development that are then lost in adulthood (Stanfield et al., 1982; O'Leary and Terashima, 1988; Low et al., 2008). Therefore, it appears that subcortical projections implement a common blueprint of projections independent of their areas, as if layer 5 neurons do not adopt areal identities at the early stage of development but are instead sculpted later depending on their origins (O'Leary and Koester, 1993). Concurrently, data are emerging that early genetic instructions frame the development of later emerging functional areas of the neocortex, such as the visual, somatosensory, and motor areas (O'Leary et al., 2007; Joshi et al., 2008; Arai and Pierani, 2014; Zembrzycki et al., 2015). These areas are distinct from each other in terms of their function as well as the underlying neuronal circuits.

In the nervous system, the Eph family of receptor tyrosine kinases are involved in various functions such as axon guidance, cell distribution, and synapse formation (Egea and Klein, 2007; Lai and Ip, 2009; Niethamer and Bush, 2019). The interaction of Eph receptors with its ligand, Ephrins (Efn), on an adjacent cell surface introduces both forward signaling on the receptor-expressing membrane region and reverse signaling on the ligand-containing membrane region (Egea and Klein, 2007). It is known that within a single modality that constitutes the corticothalamic pathway (e.g., within the somatosensory cortex), gradient expression of Eph receptor contributes to topographic connection according to the gradient expression of the Efn in the target (Torii and Levitt, 2005). We here asked whether this signal is involved in the regional organization of corticopontine projection.

Materials and Methods

Animals. C57BL/6JJmsSlc (SLC; catalog #5488963, MGI; RRID:MGI:5488963) and ICR (SLC; catalog #5462094, MGI; RRID:MGI:5462094) mice were used. *Fezf2*-tdTomato mouse was obtained from the Mutant Mouse Regional Resource Center [MMRRC; Stock Tg (*Fezf2*-tdTomato) SZ89Gsat/Mmucd; stock #036540-UCD], a National Center for Research Resources-National Institutes of Health-funded strain repository, and had been donated to the MMRRC by the National Institute of Neurological Disorders and Stroke-funded GENSAT BAC Transgenic Project. The day of confirmation of a vaginal plug was designated as embryonic day 0.5 (E0.5). The day of birth was designated as postnatal day 0 (P0). All pregnant animals used for the *in utero* electroporation method were deeply anesthetized by intraperitoneal injection of mixture of medetomidine (0.3 mg/kg), midazolam (4 mg/kg), and butorphanol (5 mg/kg). All experiments were conducted in compliance with the guidelines for the use of laboratory animals of University of Fukui and Osaka University, and were approved by the Animal Research Committee of the University of Fukui and the Animal Experimentation Committee of Osaka University. All possible efforts were made to minimize the number of animals used and their suffering.

Generation of EphA7 *knock-out mouse (*EphA7$^{-/-}$ *mouse).* pX330-U6-Chimeric_BB-CBh-hSpCas9 vector was a gift from Feng Zhang (Addgene plasmid #42230; Cong et al., 2013). *EphA7*$^{-/-}$ mice were generated by the CRISPR-Cas9 system using the pX330-U6-Chimeric_BB-CBh-hSpCas9 vector that was inserted with the following target guide RNA sequence: 5′-UGCACACACGGGGGAGGCGCAGG-3′ (the protospacer adjacent motif sequence is underlined). This plasmid was injected into the fertilized eggs that were then transferred into the oviduct of pseudopregnant ICR female (Mashiko et al., 2013). Born pups were checked by PCR amplification and sequencing of the target locus. We selected *EphA7*$^{-/-}$ mice with indel mutation at nucleotide position 71 in the coding site (CDS), 13 bp deletion plus 3 bp insertion, which resulted in frame shift mutation and a premature stop codon.

Antibodies. The following primary antibodies were used: rat anti-Ctip2 (1:500; catalog #ab18465, Abcam; RRID:AB_2064130), goat anti-EphA7 (1:250; catalog #AF608, R&D Systems; RRID:AB_2099680), chicken anti-EfnA5 (1:250; catalog #GW21054, Sigma-Aldrich; RRID:AB_1848025), chicken anti-GFP (1:1000; catalog #ab13970, Abcam; RRID:AB_300798), rabbit anti-FLAG (1:400; catalog #F7425, Sigma-Aldrich; RRID:AB_439687), mouse anti-V5 (1:400; catalog #R960-25, Thermo Fisher Scientific; RRID:AB_2556564), rabbit anti-β-actin HRP conjugated (1:5000; catalog #PM-053–7, MBL; RRID:AB_10697035), mouse anti-α-tubulin HRP conjugated (1:1000; catalog #PM054-7, MBL; RRID:AB_10695326), mouse anti-Tau1 PC1C6 antibody (1:250; catalog #MAB3420, Millipore; RRID:AB_11213630), and rabbit anti-RFP antibody (1:250; catalog #PM005, MBL; RRID:AB_591279). The following secondary antibodies were used: HRP-conjugated donkey anti-goat IgG (1:5000; catalog #sc-2020, Santa Cruz Biotechnology; RRID:AB_631728), HRP-conjugated goat anti-chick IgY (1:5000; catalog #sc-2428, Santa Cruz Biotechnology; RRID:AB_650514), donkey anti-rat IgG H&L (Biotin) preadsorbed (1:1000; catalog #ab102259, Abcam; RRID:AB_10711708), Alexa Fluor 488- and Alexa Fluor 568-conjugated secondary antibodies [1:500; catalog #A-11001 (RRID:AB_2534069), catalog #A-11004 (RRID:AB_2534072), catalog #A-11008 (RRID:AB_143165), and catalog #A-11011 (RRID:AB_143157), Thermo Fisher Scientific], and Alexa Fluor 647-conjugated secondary antibodies (1:500; catalog #ab150175, Abcam; RRID:AB_2732800)

In situ *hybridization.* cDNA fragments of mouse *EphA7* and *EfnA5* were amplified by RT-PCR with primers 5′-GAAGTAACATTGG ATACATGCCCCA-3′ and 5′-TTGGGATGCTCCGGCTCCT-3′ (for *EphA7*); 5′-CTTTTGGCAATCCTACTGTTCC-3′ and 5′-TGCTCACT

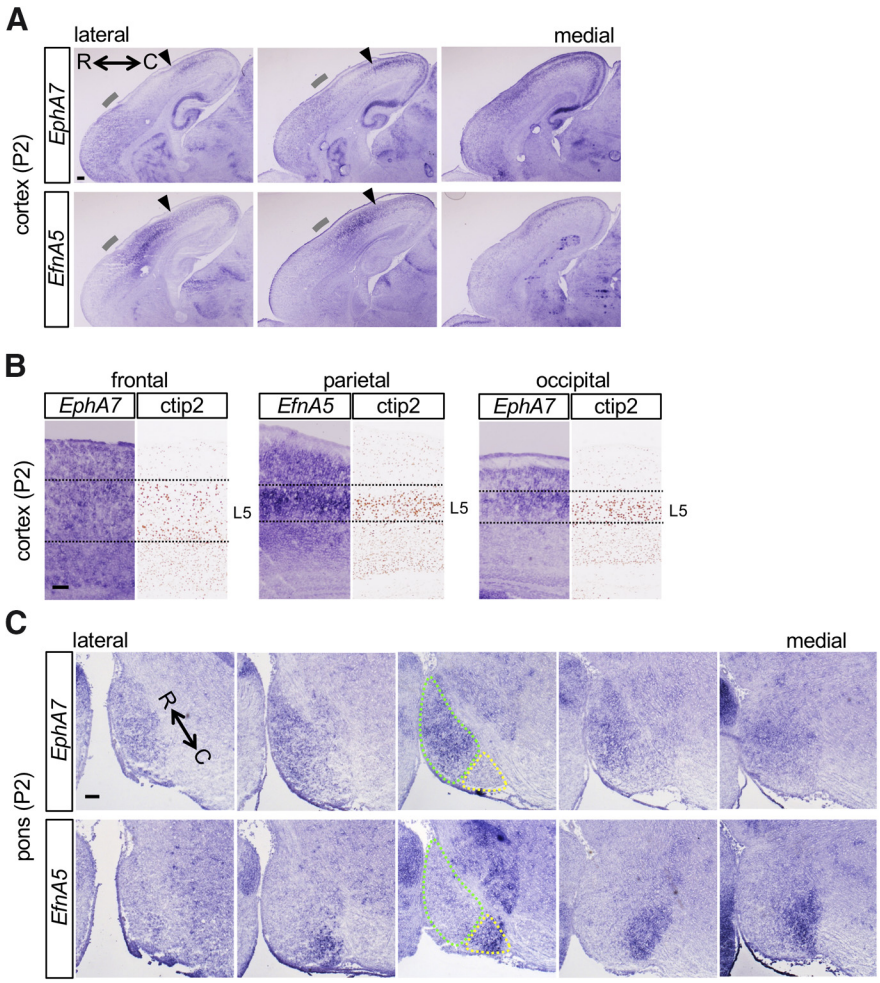

Figure 1. *EphA7* and *EfnA5* are expressed in the cortex and the BP in a region-specific and mutually exclusive manner. ***A–C***, Parasagittal sections; anterior (rostral) left and posterior (caudal) right. *EphA7* and *EfnA5* were expressed in a mutually exclusive manner both in layer 5 (L5) of the cerebral cortex (***A***, ***B***) and the BP (***C***). Arcs and arrowheads in ***A*** indicate boundaries of *EphA7*- and *EfnA5*-expressing cortical regions. ***C***, The *EphA7*-expressing area in the BP is surrounded by a green dotted line, whereas the *EfnA5*-expressing area is surrounded by a yellow dotted line. Scale bars, 100 µm. R, Rostral; C, caudal.

TCCACACTCCTAGA-3′ (for *EfnA5*); and cloned into the pGEM-T vector (catalog #A1360, Promega) as templates for probe synthesis. *In situ* hybridization was performed with DIG-labeled RNA probes as described previously (Tiong et al., 2019). In brief, hybridization was performed with the probe in 50% formamide, 5× SSC, and 200 μg/ml yeast tRNA for 16 h at 55°C. High-stringency wash steps were as follows: 5× SSC, 20 min at room temperature (RT); 2× SSC, 20 min at 65°C; and two washes with 0.2× SSC, 20 min at 65°C. After blocking with the 1% blocking reagent (Roche) in PBS for 45 min at RT, detection was performed with anti-DIG-AP (1:1000; catalog #11093274910, Roche; RRID: AB_514497) overnight at 4°C, and subsequently visualized using the NBT/BCIP (nitro blue tetrazolium chloride/5-bromo-4-chloro-3-indolyl phosphate) solution (Roche) overnight at RT. Images were captured using an upright microscope (model BX-50, Olympus).

Vectors. pCAGGS vector (Niwa et al., 1991) was modified to insert a customized multiple cloning site with or without a C-terminal 3xFLAG tag (pCAGGS-5MCS or pCAGGS-5MCS-FLAG, respectively). The full-length mouse *EphA7* CDS [National Center for Biotechnology Information (NCBI) sequence ID: NM_010141.4) and *EfnA5* CDS (NCBI sequence ID: NM_207654.2) were amplified by PCR from cDNA of E14.5 mouse brain using specific primers for mouse *EphA7* (5′-atacagatctgccaccATGGTTGTTCAAACTCGGT TCCCTTCG-3′ and 5′-atacgatatcCACTTGGATGCCTGTTCCGTG TAAATGC-3′) and for mouse *EfnA5* (5′-atacagatctgccaccATGTTG CACGTGGAGATGTTGACGC-3′ and 5′- atacgatatcTAATGTCA AAAGCATCGCCAGGAGGAAC-3′), and cloned into the BglII/EcoRV site of pCAGGS-5MCS or pCAGGS-5MCS-FLAG vector. Expression vectors of full-length mouse *EphA7* containing 5′ UTR and 3′ UTR [Clone ID: pCS6 (BC06153)] and full-length mouse *EfnA5* containing 5′ UTR and 3′ UTR [Clone ID: pCS6 (BC040218)] were purchased from Trans Omic. EfnA5-AP vector (Serizawa et al., 2006) was a gift from Hitoshi Sakano (University of Fukui, Japan) and Haruki Takeuchi (The University of Tokyo, Japan). For the construction of EphA7-AP vector, the EphA7 sequence (1662 bp coding 1–554 aa) was amplified from pCAGGS-EphA7-FLAG vector by PCR and inserted into the NheI/HindIII site of APtag-5 vector (catalog #QV5, GenHunter). For the construction of pCAGGS-EfnA5-V5 vector, the V5 tag was inserted before the glycosylphosphatidylinositol (GPI) anchor signal. The EfnA5 sequence upstream of the GPI anchor signal tagged by V5, and the remaining EfnA5 sequence containing GPI anchor signal were amplified from pCAGGS-EfnA5 vector by PCR using the following primers: 5′-GGCCGCG AATTCGATATCgccaccATGTTGCACGTGGA GATGTTGAC-3′ and 5′-GAGGAGAGGGT TAGGGATAGGCTTACCGGTGTCATCTGCT GGTTCTAATGAATTTTC-3′; 5′- CCTAA CCCTCTCCTCGGTCTCGATTCTACGGT ACATGAGTCAGCCGAGCCATC-3′ and 5′- CAGTCACTCGAGGATATCCTATAATGTC AAAAGCATCGCCAGGAG-3′. These two PCR products were inserted into the EcoRV site of pCAGGS-5MCS vector using In-Fusion HD Cloning Kit (catalog #639648, Clontech). Plasmids vector for short hairpin RNA (shRNA) constructs were obtained from the MISSION RNAi Consortium shRNA Library (Sigma-Aldrich). The targets of shRNAs for each gene were as follows: pLKO.1-shEphA7-#1, 5′-CGGAAGTAACATT GGATACAT-3′; pLKO.1-shEphA7-#2, 5′-CC ACCCAAATGTCGTCCATTT-3′; pLKO.1-shEphA7-#3, 5′-CCG GCAGGAATATACGAGAAA-3′; pLKO.1-shEphA7-#4, 5′-CTG AGTCTCCAAGAGAATTCTTC-3′; pLKO.1-shEphA7-#5, 5′-CCTAA GTGCCACCAGAATATA-3′; pLKO.1-shEfnA5-#1, 5′- CGTGTTTATC TGTGGGAGATA-3′; pLKO.1-shEfnA5-#2, 5′- CCAACAAATGA CACCGTACAT-3′; pLKO.1-shEfnA5-#3, 5′- GTCAGGACAGT AAGGTGATTG-3′; pLKO.1-shEfnA5-#4, 5′- CCACACGTCCA AAGGGTTCAA-3′; and pLKO.1-shEfnA5-#5, 5′- CCGAGAGT ATTTCTACATCTC-3′. The control vector (pLKO.1-shScramble) was constructed by insertion of an oligonucleotide containing the sequence 5′-CCTAAGGTTAAGTCGCCCTCG-3′ into the pLKO.1-puro vector.

In utero *electroporation. In utero* electroporation-mediated gene transfer into cortical neurons or pontine nucleus neurons was performed essentially as described previously (Nagano et al., 2002; Zhu et al., 2009; Iguchi et al., 2012). In brief, pregnant ICR mice were deeply anesthetized before the experiments. Approximately 1–2 µl of plasmid DNA purified using a NucleoBond Xtra Maxi EF (catalog #740424.50, MACHEREY-NAGEL) in PBS (2.0–3.5 µg/µl) together with Fast Green (final concentration, 0.01%), was injected into the lateral ventricle or the fourth ventricle of the male and female embryos with a glass micropipette (catalog #GD-1.5, Narishige). The relative ratios of each plasmid in the mixed solution were as follows: pCAGGS-tdTomato: pLKO.1-shRNA vector = 1:3; pCAGGS-tdTomato: pCAGGS-EphA7-FLAG or pCAGGS-

EfnA5-V5 vector = 1:3; pCAGGS-EGFP: pCAGGS-5MCS or pCAGGS-EfnA5-V5 vector = 1:3; and pCAGGS-mTsapphire: pCAGGS-EphA7-FLAG vector = 1:3. After soaking the uterine horn with PBS, the head of the embryo was pinched with a forceps-type electrode (CUY650P5, CUY650P3, NEPAGENE), and five cycles of square electric pulses (E12.5 cortex: 34 V, 50 ms duration with 950 ms intervals; E12.5 rhombic lip: 37 V, 50 ms duration with 150 ms intervals) were delivered using an electroporator (CUY21EDIT, NEPAGENE). Uteri were placed back into the abdominal cavity to allow the embryos to continue normal development.

Tracer injection, tissue preparation, and immunohistochemistry. For the tracing of corticospinal tract and axon collaterals, P1 mice were anesthetized on ice, and a 10% DiI (catalog #D-3883, Thermo Fisher Scientific) solution in dimethylformamide was injected into the appropriate area of the cortex by pulled glass pipettes attached to a pressure injector (picospritzer II, Parker Instrumentation). After 24 h, brains were harvested and used for sectioning and further analyses. To analyze axon collaterals, brains were harvested at P2 and fixed overnight with 4% paraformaldehyde (PFA) in PBS, placed in an agar solution (1.5% agar, 8% sucrose), cut parasagittally into 100-μm-thick sections using a microslicer (model DTK-1000, Dosaka EM). For immunohistochemical staining, fixed brains were immersed in 30% sucrose in PBS until the brains sank, embedded in OCT (optimal cutting temperature) compound (Sakura Finetechnical), and 16-μm-thick parasagittal cryosections were prepared. The sections were air dried for 30 min, and antigen retrieved in 0.01 M sodium citrate buffer, pH 6.0, by heating just below the boiling point with a microwave oven. After being incubated in the blocking buffer (10% normal donkey serum, 0.25% Triton X-100 in PBS) for 2 h at RT, sections were incubated with primary antibody in the blocking buffer overnight at 4°C. Sections were washed three times for 20 min with PBS and incubated with secondary antibody in the blocking buffer for 2 h at RT. For the detection of the biotinylated secondary antibody, Elite ABC IgG kit (Vector Laboratories) and DAB Detection Kit (Vector Laboratories) were used. Images were captured using a fluorescence microscope (AxioObserver A1, Carl Zeiss) and spinning disk confocal super resolution microscope (SpinSR10, Olympus), and were analyzed with ImageJ software (NIH; RRID:SCR_003070).

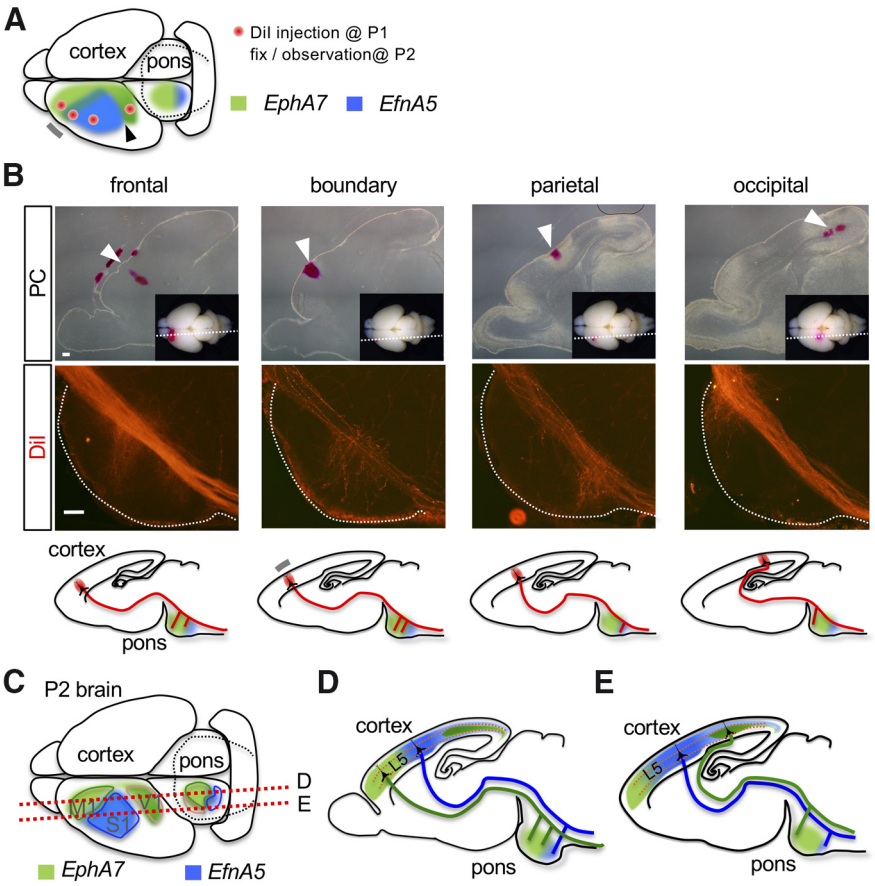

Figure 2. Region-to-region specific projection from the cortex to the BP where *EphA7* and *EfnA5* are expressed in a mutually exclusive manner. ***A***, A perspective image of expression patterns of *EphA7* and *EfnA5* in layer 5 of the cerebral cortex and the BP at P2. DiI injection sites are indicated by red dots. ***B***, Top panels, Phase contrast (PC) parasagittal images of the brain. DiI-injected sites are shown by white arrowheads. Inset images show DiI injected sites and the cutting planes (white dotted lines). Middle panels, Axon collaterals in the BP traced by DiI. Bottom panels, Summary of the results. ***C***, A perspective image of expression patterns of *EphA7* and *EfnA5* in layer 5 of the cerebral cortex and the BP at P2. ***D***, ***E***, Region-to-region specific projection from the cortex to the basilar pons at P2. Cutting planes of ***D*** and ***E*** are shown in red dotted lines in ***C***. Scale bars, 100 μm.

Alkaline phosphatase-tag protein binding assay. Binding assay was performed with conditioned media from the HEK293T cell transfected with alkaline phosphatase (AP)-tag protein expression vector, as described previously (Flanagan and Leder, 1990; Cang et al., 2005). In brief, 18 μm fresh-frozen sections were air dried for 2 h at RT, fixed in 100% methanol for 20 s at −20°C, washed in HEPES-buffered saline (HBS; 10 mM HEPES, pH 7.0, 150 mM NaCl), rinsed twice in HBAH solution (HBSS, 0.5 mg/ml BSA, 20 mM HEPES, pH 7.0), hybridized with the AP-tagged protein for 90 min at RT. Sections were washed six times in cold HBAH, fixed in acetone-formalin fixative [65% (v/v) acetone, 8% (v/v) formalin, 20 mM HEPES, pH 7.0] for 15 s, washed twice in HBS, then incubated in preheated HBS in a 65°C water bath for 15 min. After being washed in AP staining buffer (100 mM NaCl, 5 mM $MgCl_2$, 100 mM Tris-HCl, pH 9.5), the sections were proceeded for detection with the NBT/BCIP (Roche) in AP staining buffer overnight at RT. The reaction was stopped in PBS with 10 mM EDTA, and sections were fixed in 8% (v/v) formalin for 20 min and stained by DAPI (catalog #D523, Dojindo) in PBS with 10 mM EDTA. Images were captured using a microscope (model BZ-X710, KEYENCE).

Collapse assay. Neurons from E14.5 cortex that had been electroporated with pLKO.1-shRNA vector together with pCAGGS-tdTomato vector at E12.5, were cultured in a four-well chamber cover (catalog #SCC-004, MATSUNAMI) coated with polyethyleneimine (PEI; catalog #P3143, Sigma-Aldrich) at 1×10^5 cells/well. At 4 d *in vitro* (DIV4), neurons were treated with 257 ng/ml recombinant hFc (catalog #009–000-008, Jackson ImmunoResearch; RRID:AB_2337046) or 500 ng/ml recombinant EfnA5-hFc (catalog #374-EA-200, R&D Systems). After incubation for 20 min at 37°C, neurons were fixed in 4% PFA/4% sucrose in PBS for 15 min at RT and stained with Phalloidin-iFluor 488 Reagent (1:1000; catalog #ab176753, Abcam). Images were captured using a fluorescence microscope (model BZ-X710, KEYENCE). The percentage of collapsed growth cones was measured by blinded procedure. Collapsed growth cone was defined by the absence of lamellipodia with F-actin at the tips of neurite.

Stripe assay with rostrocaudally fully spanning-cortical slices. Stripe patterns were produced as described previously (Weschenfelder et al., 2013; Yamagishi et al., 2016). Twenty-six micrograms per milliliter recombinant hFc or 51 μg/ml recombinant EfnA5-hFc was fluorescently labeled and clustered by mixing with 150 μg/ml Alexa Fluor-647-conjugated anti-human IgG (catalog #A-21445, Thermo Fisher Scientific; RRID:AB_2535862) in PBS for 30 min at RT and used for the first stripe. Twenty-six micrograms per milliliter recombinant hFc was mixed with

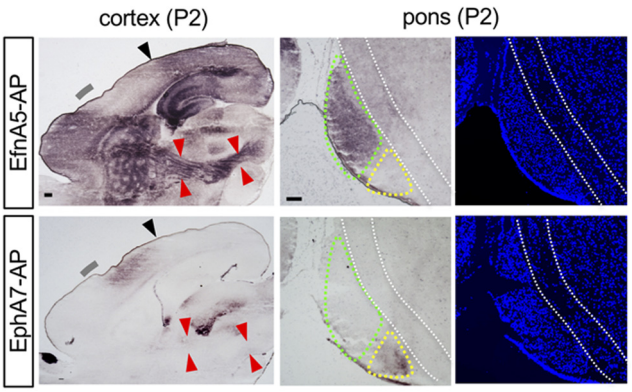

Figure 3. EfnA5 protein-binding sites exhibit similar distribution patterns with the expression of *EphA7*. EfnA5-AP and EphA7-AP binding sites on the cortex (left panels) and the pons (middle panels) were shown. Gray arcs and black arrowheads in left panels indicate boundaries between EfnA5-AP and EphA7-AP binding sites on the cortex. The internal capsule and the cerebral peduncle are indicated by red arrowheads. The EfnA5-AP binding site in the BP is surrounded by a green dotted line, whereas the EphA7-AP binding site is surrounded by a yellow dotted line. Corticospinal axonal main shaft is shown by two white dotted lines. DAPI staining of the BP (right panels). Scale bars, 100 μm.

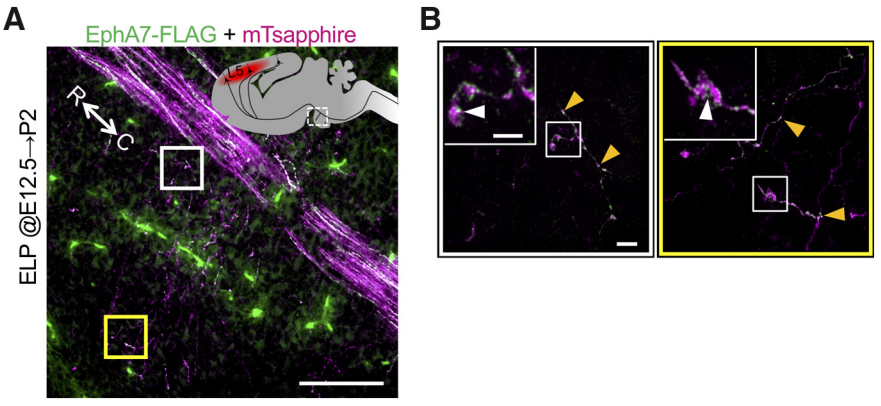

Figure 4. EphA7 protein localizes in the growth cone of the axon collaterals. ***A***, ***B***, EphA7 was localized in the growth cones of axon collaterals as well as in the axonal main shafts of the corticospinal tract. Localization of EphA7-FLAG assessed by immunohistochemistry against FLAG (green) at P2. An expression plasmid of mTsapphire together with that of EphA7-FLAG was transfected into the layer 5 corticospinal neurons at E12.5. mTsapphire was stained with anti-GFP antibody (magenta) to visualize the axonal shaft and collateral branches. Noted that the blood vessel was stained nonspecifically in the BP. ***B***, High-magnification images of the white and yellow squares in ***A***. Insets show higher-magnification images in the square. EphA7 was localized in clusters in the axonal shaft (orange arrowheads) and growth cones (white arrowheads) of the axon collaterals. Scale bars: ***A***, 100 μm; ***B***, 2 μm; ***B***, inset, 1 μm. R; rostral, C; caudal.

150 μg/ml unconjugated goat anti-human IgG (catalog #I2136, Sigma-Aldrich; RRID:AB_260147) and kept on ice until preparation of the second stripe. For the first stripe preparation, protein mixture was injected into the slit of the matrix (channel width, 90 μm parallel; product code 2A, Silicone Matrices) on the PEI-coated 6 cm culture dish, incubated for 30 min at 37°C, and washed three times with PBS. For the second stripe preparation, the matrix was removed and the striped area was covered with nonlabeled hFc for 30 min at 37°C, washed three times with PBS, and then coated with 20 μg/ml laminin (catalog #120–05751, Wako) in PBS for 1 h at 37°C. After washing three times with PBS, 3 ml of culture medium (Neurobasal medium, catalog #21103049, Thermo Fisher Scientific), 1× B-27 (catalog #17504044, Thermo Fisher Scientific), 2 mM GlutaMAX (catalog #35050061, Thermo Fisher Scientific), 100 U/ml penicillin, and 0.1 mg/ml streptomycin) was added and kept in incubator until use.

For rostrocaudally fully spanning (RCFS) cortical slice preparation, whole brain was harvested from *Fezf2*-tdTomato mice at P0. Meninges were removed, and cortical slices containing the frontal, parietal, and occipital cortices were cut out at ~0.5 mm thickness by microscissors. White matter was removed from a cortical slice using an MVR V-Lance Knife (catalog #8065912001, Alcon). Cortical slices were put on the edge of the stripe and culture medium was decreased to 1.5 ml to enhance the attachment of the slice to the culture dish. After 2 d, culture medium was added up to 3 ml, and the axon projection pattern was analyzed at DIV4. Cortical explants were fixed in 4% PFA/4% sucrose in PBS for 20 min at RT and stained with anti-Tau1 PC1C6 antibody and anti-RFP antibody. Images were captured using a fluorescence microscope (model BZ-X710, KEYENCE).

Experimental design and statistical analyses. Vibratome sections used for quantification of collateral formation were made at an angle that included the entire corticospinal tract and axon collaterals in the basilar pons (BP). For the picture data, a representative of more than three picture data was shown in each figure. For the analysis of the distribution of *EfnA5* expression in the rostrocaudal axis of the cortex, *in situ* hybridization images were analyzed using ImageJ. Grayscale images were inverted so that *in situ* hybridization signals were shown in white. Signal intensities along the rostrocaudal axis were measured. A mean gray value was calculated for each 5% of the rostrocaudal length. These values were converted to the percentage of maximal intensity within each section so that relative values could be compared between animals and across genotypes. For the analysis of stripe assay, each cortical slice was divided into the three areas (frontal, parietal, occipital) so that each contained nine pairs of stripes. Using ImageJ, the fluorescence intensity of Tau1-positive axons was measured. 50 × 400 pixels rectangle, of which size was fit to each stripe, was used as an ROI for the measurement. The nearest side of the rectangle to the cortical slice was 100 pixels apart from the bottom edge of the cortical slice. Eighteen rectangles could be found for each area (frontal, parietal, occipital), and the middle 10 rectangles were used for further measurement so that border areas were not included. The fluorescence ratios of neighbor rectangles were calculated. For the analysis of directionality of the axon collaterals projecting to the BP, the images obtained were rotated so that the main shaft of the corticospinal tract was horizontal, and the region of the BP, which includes axon collaterals, was manually surrounded as an ROI. Using the Directionality plugin of ImageJ, a histogram of the angle component included in the ROI was created, and the highest peak was fitted by a Gaussian function. The center of the Gaussian was calculated as the preferred direction value, and the SD of the Gaussian was calculated as the dispersion of direction (Liu, 1991; Sensini et al., 2018). For the analysis of the distribution of axonal collaterals along the rostrocaudal axis of the BP, the regions of the BP just beneath the corticospinal axonal shaft were divided into 10 bins along the rostrocaudal axis. The ratio of the fluorescence intensity of each bin to the total fluorescence intensity of all bins was analyzed with ImageJ. For statistical analysis, data analysis was performed using the JMP Pro 15 (SAS). We used Welch's *t* test to verify whether the means of the two datasets were significantly different. For multiple comparisons, we performed a Tukey–Kramer test or Dunnett's test. The significance threshold was set at $p < 0.05$. In bar graphs, all data are plotted as the mean ± SEM.

Results

EphA7 and *EfnA5* are expressed in the cortex and the basilar pons in a region-specific and mutually exclusive manner

To examine whether Eph receptor signals are involved in the formation of the regionally organized corticofugal projections, we first examined the expression patterns of *EphA7* and its binding

partner *EfnA5* (Janis et al., 1999) using *in situ* hybridization analysis on parasagittal sections of mouse P2 brain (Fig. 1*A–C*). Consistent with previous reports (Rashid et al., 2005; Miller et al., 2006), we found that *EphA7* was expressed in frontal and occipital areas of the cortex and that *EfnA5* was expressed in the parietal area of the cortex (Fig. 1*A*). *EphA7* and *EfnA5* were exclusively expressed in layer 5 of the cerebral cortex (Fig. 1*A*,*B*). The boundary between the *EfnA5* expression and *EphA7* expression in the caudal region of the cortex was clear, while that in the rostral region of the cortex was somewhat unclear because of the lower expression of *EphA7* in the frontal cortex (Fig. 1*A*). Interestingly, *EphA7* was expressed in the BP, but, as demonstrated using *in situ* hybridization, only in the rostral two-thirds of the BP (Fig. 1*C*). Similarly, *EfnA5* and *EphA7* expression patterns also appeared to be mutually exclusive in the caudal region of the BP (Fig. 1*C*).

Organization of the corticopontine projection follows the region-specific expression of *EphA7* and *EfnA5*

We then asked whether the precise organization of the corticopontine projection corresponded to the region-specific expression of *EphA7* and *EfnA5*. To this end, we injected DiI tracer into the *EphA7*-postive frontal or occipital area, the *EfnA5*-positive parietal area, and the boundary between the frontal and parietal area (Fig. 2*A*,*B*). We found that axon collaterals originating from cell bodies in the *EphA7*-positive frontal area extended a main bundle into the rostral two-thirds of the BP (Fig. 2*B*, frontal). A subset of these axon collaterals extended as a bundle into the BP near the boundary of mutually exclusive *EphA7* and *EfnA5* expression (Figs. 1*C*, 2*B*, frontal). This bundle was more evident when we traced from cortical neurons located in the boundary of the expression of *EphA7* and *EfnA5* (Fig. 2*B*, boundary). Similarly, *EphA7*-positive cortical neurons with cell bodies in the occipital area extended their axons into the rostral and/or lateral part of the BP (Fig. 2*B*, occipital). Conversely, *EfnA5*-positive neurons in parietal cortex extended their axons into the caudal one-third of the BP (Fig. 2*B*, parietal). These results suggest that precise organization of the corticopontine projection corresponds to the region-specific expression of *EphA7* and *EfnA5* (Fig. 2*B–E*).

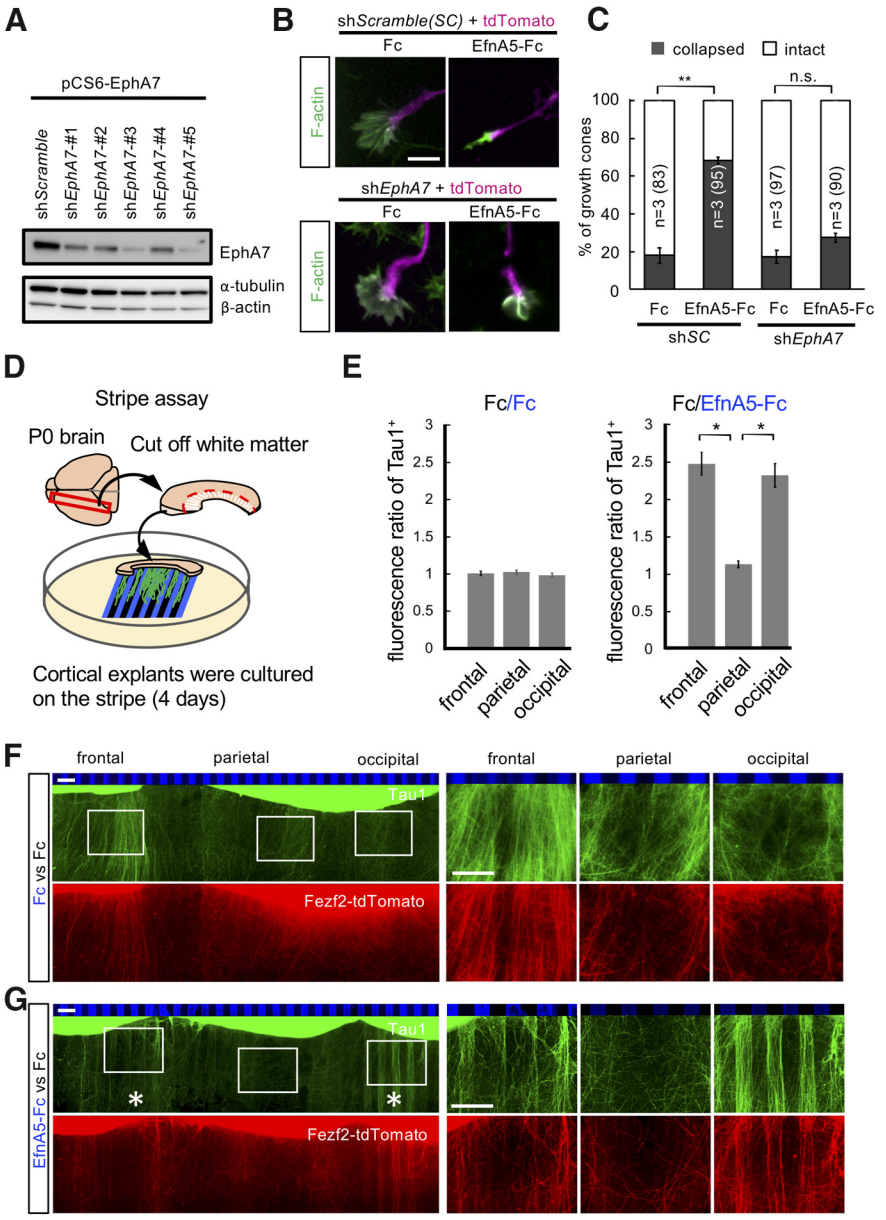

Figure 5. EfnA5 induces growth cone collapse of layer 5 neurons in the frontal and occipital area. ***A***, KD efficiency of EphA7-KD vectors. KD efficiency was evaluated by immunoblotting using the HEK293T cell lysate, which expressed EphA7 together with shRNA vectors. sh*EphA7*-#5 was used for *in vivo* KD experiments because of the highest KD efficiency. Tubulin and actin were loading controls. ***B***, Representative images of growth cone morphology of cortical layer 5 neurons prepared from E14.5 embryo (electroporated at E12.5) at DIV4. Frontal neurons were targeted for electroporation. Scale bar, 10 μm. ***C***, EfnA5-Fc did not induce noticeable growth cone collapse in EphA7 KD neurons. *n* indicates the number of independent experiments. Numbers of analyzed growth cones are shown in brackets. Values are the mean ± SEM. Tukey–Kramer test, $^{**}p < 0.01$, n.s. not significant. ***D***, Experimental procedures for stripe assay with the RCFS cortical slices. Cortical slices were taken from P0 *Fezf2*-tdTomato mice, in which tdTomato was expressed in the corticospinal neurons. ***E***, Fluorescence ratio of Tau1-positive corticospinal axons between the two distinct stripes. Frontal, Axons from the frontal area; parietal, axons from the parietal area; occipital, axons from the occipital area. Values are the mean ± SEM. Tukey–Kramer test, $^{*}p < 0.05$. ***F***, ***G***, Axons from the frontal area and the occipital area elongated preferentially on the Fc lanes (black lanes), but not on stripes of EfnA5-Fc (blue lanes). Right panels show magnified images of the white squares in the leftmost panels. Typical preference cases are indicated with asterisks. Scale bars, 200 μm.

Distribution of EfnA5 protein-binding areas is similar to the *EphA7*-expressing regions

A protein of interest tagged with AP is sometimes used as a ligand for visualization of its binding partner. To elucidate the localization of the EfnA5 and EphA7 binding partner, we generated Efn5-AP and EphA7-AP. We then found that the localization patterns of EfnA5-AP and EphA7-AP were similar to the distribution of *EphA7* and *EfnA5*, respectively (Figs. 1*A*,*C*, 3), suggesting that these molecules bind to each other in the cortex. Interestingly, we found strong EfnA5-AP binding in the internal capsule and the cerebral peduncle (Fig. 3, red arrowheads),

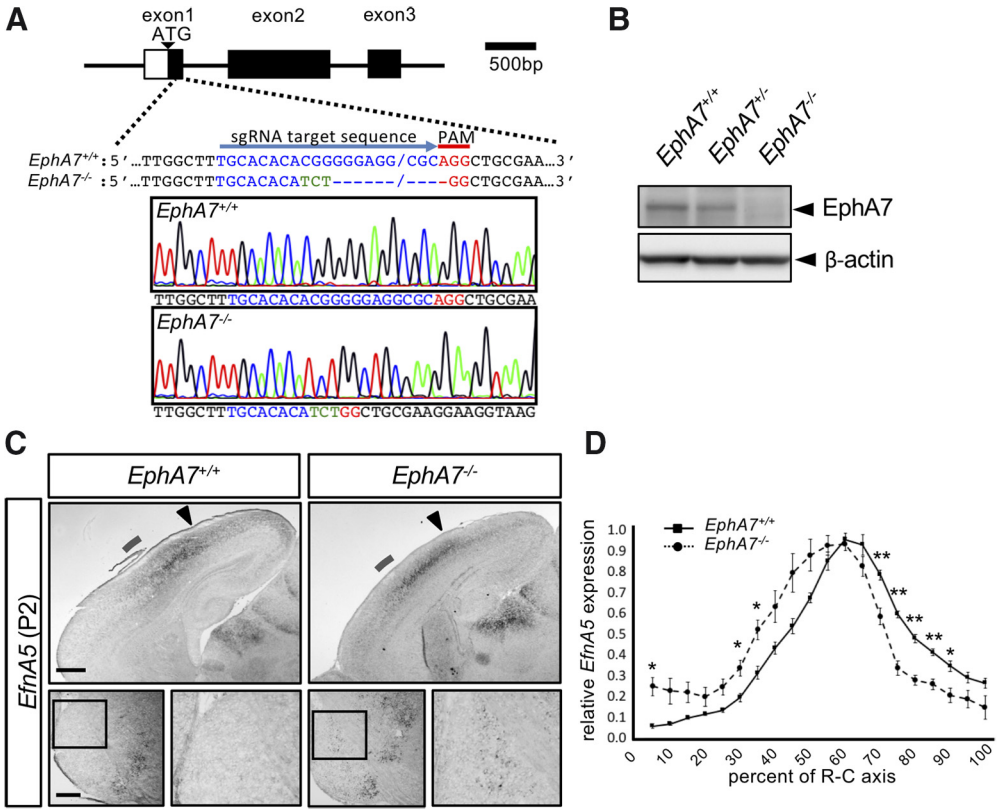

Figure 6. Generation of *EphA7*$^{-/-}$ mice. ***A***, *EphA7*$^{-/-}$ mouse was generated using the CRISPR-Cas9 system. A knock-out allele was created by the frame shift insertion (green)/deletion (–; indel) mutations, which leads to the appearance of a premature stop codon. ***B***, Mouse brain lysates from each genotype at P2 were subjected to immunoblotting. ***C***, Expression patterns of *EfnA5* in the cortex (top) and the BP (bottom) of the *EphA7*$^{+/+}$ and the *EphA7*$^{-/-}$ mice were examined by *in situ* hybridization. Magnified images of rectangles in bottom left panels were shown in the right panels for each genotype. Ectopic *EfnA5* expression was observed in the rostral region of the BP of *EphA7*$^{-/-}$ mice. Scale bars, 100 μm. ***D***, Relative *EfnA5* expression profiles through the rostrocaudal axis of the cortex. The *EfnA5*-expressing cortical region was slightly expanded with a shift to the anterior (rostral) in *EphA7*$^{-/-}$ mice. Values are the mean ± SEM. Welch's *t* test: $*p < 0.05$, $**p < 0.01$. *EphA7*$^{+/+}$, $n = 4$; *EphA7*$^{-/-}$, $n = 4$.

whereas we found low binding in the corticospinal tract near the BP (Fig. 3, middle, white dotted lines).

EphA7 protein is localized in the growth cones of the axon collaterals

We next examined whether EphA7 was present in the growth cones of axon collaterals and in the axonal main shafts of the corticospinal tract. Because EphA7-specific antibodies were not available, we had EphA7 fused with a FLAG epitope exogenously expressed in layer 5 corticospinal neurons at E12.5 (Fig. 4*A*,*B*). We found that exogenous EphA7 was localized in clusters in corticospinal tract axonal shafts and in tips of axon collaterals (Fig. 4*A*,*B*).

Growth cones of corticospinal neurons in the frontal or occipital area collapse in response to EfnA5

We asked whether corticospinal neurons respond to EfnA5 in an EphA7-dependent manner. To confirm the response of endogenous EphA7 in the axonal growth cone, we then performed collapse assays in primary cultured cortical neurons in which layer 5 neurons were labeled with tdTomato through *in utero* electroporation at E12.5. We found that recombinant EfnA5 was capable of eliciting growth cone collapse of a large number of layer 5 neurons (Fc: 18.1 ± 4.07%, $n = 3$, 83 cells; EfnA5-Fc: 68.4 ± 1.74%, $n = 3$, 95 cells; Tukey–Kramer test, $p < 0.0001$) but had little effect on EphA7-knock-down (KD) neurons (Fc: 17.3 ± 3.37%, $n = 3$, 97 cells; EfnA5-Fc: 27.5 ± 2.45%, $n = 3$, 90 cells; Tukey–Kramer test, $p = 0.16$; Fig. 5*A*–*C*). These results suggest that EphA7 receptors are transported from the cortex along the corticospinal axon shaft to axonal growth cones of collaterals extending in the BP, and that EfnA5 likely functions as the ligand that repulses EphA7-positive growth cones.

We next asked in what way EfnA5 impacted axonal extensions of layer 5 neurons. To address this question, we conducted stripe assays with RCFS cortical slices. First, we took the whole cortex at P0 out of *Fezf2*-tdTomato mice, which express tdTomato in layer 5 corticospinal neurons, made cortical slices spanning from the rostral to the caudal end of the cortex, and placed these on culture dishes where control Fc (black stripes) and EfnA5-Fc (blue stripes) were plated on alternating stripes. To make axons extend straight out of the slices along the stripes so that we could observe axonal extensions clearly, we removed the white matter where axons make a turn before placing the slices onto the culture dishes (Fig. 5*D*). Cortical slices were observed after 4 d in culture. We found that layer 5 axonal extensions from both the frontal and occipital areas appeared irregular and/or collapsed on EfnA5-Fc stripes, whereas those from the parietal area spread on both stripes [fluorescence ratio of Tau1-positive axons on stripes (Fc/Fc): frontal, 1.01 ± 0.03, $n = 20$ stripe pairs from four slices; parietal, 1.03 ± 0.03, $n = 20$ stripe pairs from four slices; occipital, 0.98 ± 0.03, $n = 20$ stripe pairs from four slices; Tukey–Kramer test, frontal vs parietal $p = 0.86$, occipital vs parietal $p = 0.49$; fluorescence ratio of Tau1-positive axons on stripes (Fc/EfnA5-Fc), frontal, 2.48 ± 0.15, $n = 20$ stripe pairs from four slices; parietal, 1.13 ± 0.05, $n = 20$ stripe pairs

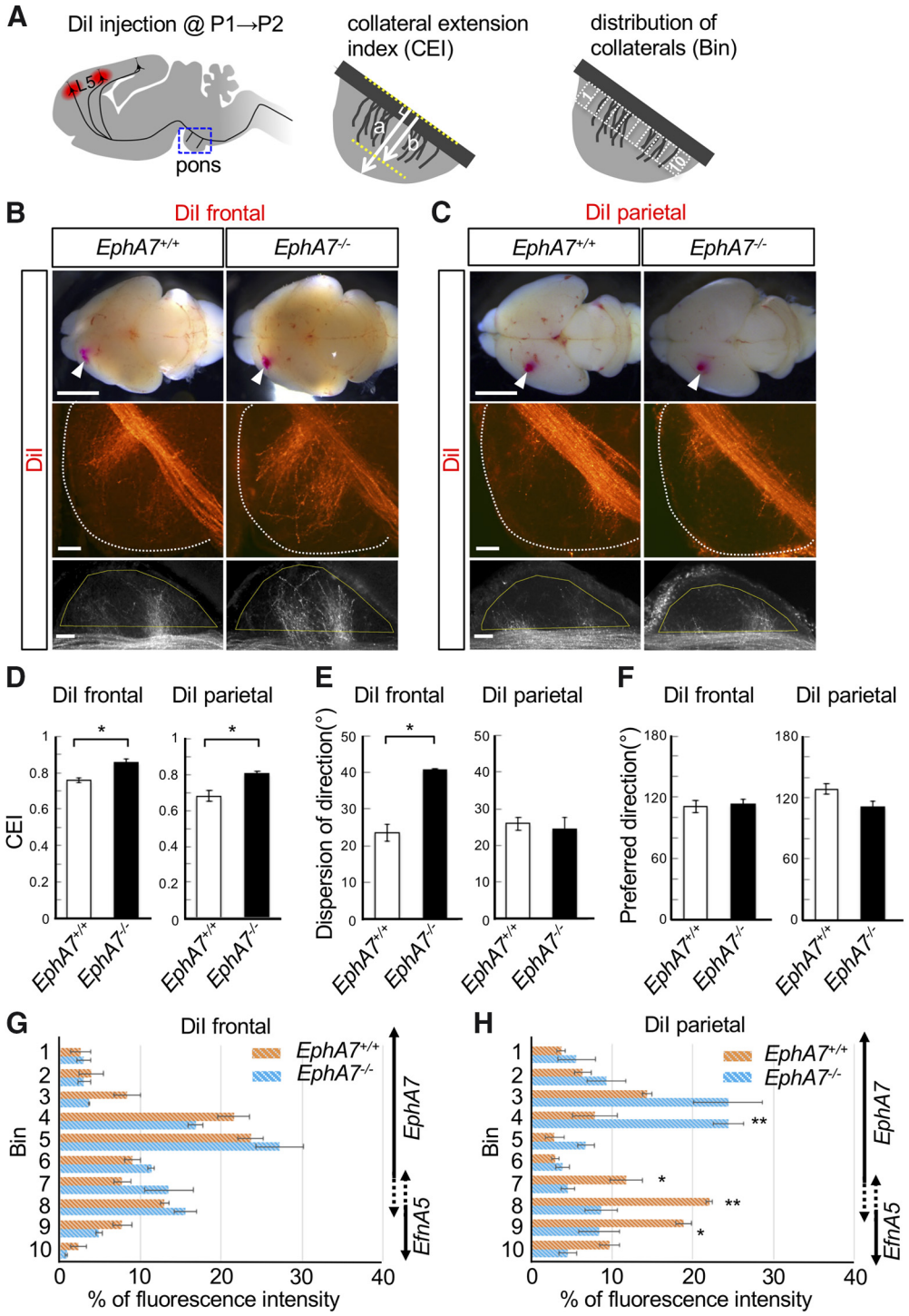

Figure 7. Dysregulated and extensive axon collateral formation in the BP of *EphA7*$^{-/-}$ mice. ***A***, Left, DiI tracer was injected into the frontal cortex or parietal cortex at P1 and the axon collaterals in the BP (pons) were observed at P2. Middle, Schematic drawing for measuring the collateral extension in the BP. We defined CEI as b/a, where b is the length of the axon collaterals from the dorsal border of the corticospinal tract, and a is the maximum distance from the border to the outer edge of the BP. Right, The regions of the BP just beneath the corticospinal axonal shaft were divided into 10 bins along the rostrocaudal axis. The ratios of the fluorescence intensity of each bin to the total fluorescence intensity of all bins were analyzed. ***B–D***, Length of the axon collaterals from the main shafts of corticospinal tract CEI (b/a) was increased in *EphA7*$^{-/-}$ mice compared with *EphA7*$^{+/+}$ mice. ***E***, Dispersion of angle component calculated from the image of axon collaterals (***B***, ***C***, bottom panels; areas surrounded by yellow lines were analyzed) was increased in the corticospinal neurons traced from the frontal cortex of *EphA7*$^{-/-}$ mice compared with *EphA7*$^{+/+}$ mice, while the preferred direction of the axon collaterals did not change in the corticospinal neurons traced from the frontal and parietal cortex. ***F***, Images in middle panels of ***B*** and ***C*** were rotated so that the main shaft of the corticospinal tract was horizontal and are shown in the bottom panels in ***B*** and ***C***. Values are the mean ± SEM. Welch's *t* test, $*p < 0.05$. DiI frontal: *EphA7*$^{+/+}$, $n = 3$; *EphA7*$^{-/-}$, $n = 3$; DiI parietal: *EphA7*$^{+/+}$, $n = 3$; *EphA7*$^{-/-}$, $n = 4$. Scale bars: 2 mm, 100 μm. ***G***, ***H***, Distribution of axonal collaterals along the rostrocaudal axis of the BP was estimated according to the fluorescence intensity in each bin. Regions of *EphA7* and *EfnA5* expression corresponding to each bin were shown on the right side of the graph. See also Figure 1*C*. Values are the mean ± SEM. Welch's *t* test: $*p < 0.05$, $**p < 0.01$. DiI frontal: *EphA7*$^{+/+}$, $n = 3$; *EphA7*$^{-/-}$, $n = 3$; DiI parietal: *EphA7*$^{+/+}$, $n = 3$; *EphA7*$^{-/-}$, $n = 4$.

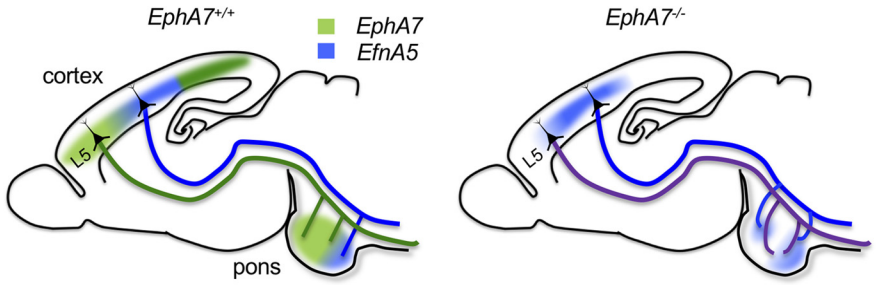

Figure 8. Summary of the corticopontine projections in *EphA7*$^{+/+}$ and *EphA7*$^{-/-}$ mice. Localization of *EphA7* (green) and *EfnA5* (blue) in layer 5 neurons and the BP, and their corticopontine projections at P2 were shown. *EphA7*$^{-/-}$ mice did not express EphA7 in either the cerebral cortex or the BP. *EfnA5*-expressing region was slightly expanded with a shift to the anterior (rostral) in the *EphA7*$^{-/-}$ mouse. Axon collaterals extended in a disorganized fashion in the BP of *EphA7*$^{-/-}$ mouse.

from four slices; occipital, 2.32 ± 0.15, $n = 20$ stripe pairs from four slices; Tukey–Kramer test, frontal vs parietal $p < 0.0001$, occipital vs parietal $p < 0.0001$; Fig. 5*E–G*]. These results suggest that the EphA7–EfnA5 inhibitory activity is working at the growth cones of extending collaterals in deciding whether to enter or avoid a certain brain area.

EphA7$^{-/-}$ mice have longer, winding, and widely spreading axon collaterals

Because evaluating collateral response solely with *in vitro* analyses can be difficult, we next created *EphA7*$^{-/-}$ mice with the CRISPR-Cas9 system to perform *in vivo* analyses (Fig. 6*A*,*B*). It is known that *EphA7* and *EfnA5* expression is mutually segregated in visual cortex (Fig. 1*A*; Miller et al., 2006). In our *EphA7*$^{-/-}$ mice, the *EfnA5*-expressing cortical region was slightly expanded with a shift to the anterior [rostral; relative EfnA5 expression in each region of rostrocaudal axis, *EphA7*$^{+/+}$ ($n = 4$) vs *EphA7*$^{-/-}$ ($n = 4$), Welch's *t* test; 5% of rostrocaudal axis, 0.06 ± 0.01 vs 0.25 ± 0.04 ($p = 0.019$); 30% of rostrocaudal axis, 0.19 ± 0.02 vs 0.33 ± 0.04 ($p = 0.025$); 35% of rostrocaudal axis, 0.31 ± 0.03 vs 0.52 ± 0.05 ($p = 0.014$); 70% of rostrocaudal axis, 0.78 ± 0.02 vs 0.58 ± 0.04 ($p = 0.008$); 75% of rostrocaudal axis, 0.59 ± 0.02 vs 0.33 ± 0.03 ($p = 0.002$); 80% of rostrocaudal axis, 0.48 ± 0.02 vs 0.28 ± 0.02 ($p = 0.001$); 85% of rostrocaudal axis, 0.41 ± 0.02 vs 0.26 ± 0.03 ($p = 0.004$); 90% of rostrocaudal axis, 0.35 ± 0.02 vs 0.21 ± 0.03 ($p = 0.018$); Fig. 6*C*,*D*]. We then examined whether the *EfnA5* expression region in the BP became expanded in the absence of EphA7, just as it does in the cortex. We found in *EphA7*$^{-/-}$ mice that *EfnA5* was expressed not only in the caudal region of the BP but also in the rostral region of the BP (Fig. 6*C*). We next studied the extension of axon collaterals toward the BP in the absence of EphA7. As a quantitative metric, we defined "collateral extension index" (CEI) as the ratio between collateral length from the dorsal border of the corticospinal tract and the maximum distance from the border to the outer edge of the BP (Fig. 7*A*, the value of b/a). When we injected DiI tracer into the frontal area of the cortex (Fig. 7*A*,*B*), we found that axon collaterals extending toward the BP were significantly longer in *EphA7*$^{-/-}$ mice compared with those of *EphA7*$^{+/+}$ mice (*EphA7*$^{+/+}$: CEI, 0.76 ± 0.02; $n = 3$ mice; *EphA7*$^{-/-}$: CEI, 0.86 ± 0.02; $n = 3$ mice; Welch's *t* test, $p = 0.03$; Figs. 7*B*,*D*, 8). Similarly, when we injected DiI tracer into the parietal area of the cortex (Fig. 7*A*,*C*), we found that axon collaterals extending toward the BP were significantly longer in *EphA7*$^{-/-}$ mice compared with those of *EphA7*$^{+/+}$ mice (*EphA7*$^{+/+}$: CEI, 0.68 ± 0.03; $n = 3$ mice; *EphA7*$^{-/-}$: CEI, 0.81 ± 0.01; $n = 4$ mice; Welch's *t* test, $p = 0.04$; Figs. 7*C*,*D*, 8). We next assessed the directionality of axon collaterals toward the BP as well as the dispersion of directionality (see Materials and Methods). We found that the preferred orientation of axon collaterals against the main shaft (as determined by the histogram of the angle component included in the ROI) did not change (DiI frontal: *EphA7*$^{+/+}$, 111.1 ± 5.7°, $n = 3$ mice; *EphA7*$^{-/-}$, 112.8 ± 5.1°, $n = 3$ mice; Welch's *t* test, $p = 0.83$; DiI parietal: *EphA7*$^{+/+}$, 128.2 ± 5.2°, $n = 3$ mice; *EphA7*$^{-/-}$, 110.7 ± 6.0°, $n = 4$ mice; Welch's *t* test, $p = 0.079$; Figs. 7*B*,*C*,*F*, 8). However, axon collaterals traced from the frontal cortex were widely dispersed in *EphA7*$^{-/-}$ mice relative to control mice (DiI frontal: *EphA7*$^{+/+}$: dispersion of direction, 24.3 ± 2.3°, $n = 3$ mice; *EphA7*$^{-/-}$: dispersion of direction, 41.6 ± 0.4°, $n = 3$ mice; Welch's *t* test, $p = 0.015$; DiI parietal: *EphA7*$^{+/+}$: dispersion of direction, 25.9 ± 1.7°, $n = 3$ mice; *EphA7*$^{-/-}$: dispersion of direction, 24.3 ± 3.2°, $n = 4$ mice; Welch's *t* test, $p = 0.68$; Figs. 7*B*, *C*,*E*, 8). Hence, the EphA7–EfnA5 axis does not appear to affect the orientation of axon collaterals, but the extent to which they spread in their target area. We next investigated the projection area of corticospinal axon collaterals in the BP. We divided regions of the BP immediately beneath the corticospinal axonal shaft into 10 bins along the rostrocaudal axis. We semiquantified the signal intensity in each bin as an estimate of abundance of collateral branches so that we could examine collateral distribution along the rostrocaudal axis (Fig. 7*A*). Axon collaterals traced from the frontal cortex were not significantly altered in the BP of *EphA7*$^{-/-}$ mice (Figs. 7*B*,*G*, 8), whereas axon collaterals traced from the parietal cortex exhibited rostrally shifted extension in the BP of *EphA7*$^{-/-}$ mice (*EphA7*$^{+/+}$, $n = 3$ mice; vs *EphA7*$^{-/-}$, $n = 4$ mice; Welch's *t* test; bin 4: 7.8 ± 2.8% vs 24.5 ± 1.9%, $p = 0.0097$; bin 7: 11.7 ± 2.0% vs 4.5 ± 0.9%, $p = 0.049$; bin 8: 22.0 ± 0.4% vs 8.6 ± 2.0%, $p = 0.0057$; bin 9: 18.8 ± 1.0% vs 8.4 ± 2.5%, $p = 0.019$; Figs. 7*C*,*H*, 8).

Projection area of the axon collaterals are controlled by EphA7 forward signaling and EfnA5 reverse signaling

To avoid any interference by ectopic EfnA5 expression because of the knockout of *EphA7* not only in the cortex but also in the BP (Fig. 6*C*,*D*), we therefore knocked down *EphA7* only in neurons of interest in the cortex and observed their phenotypes. Hence, we performed *in utero* electroporation at E12.5 to transfect KD vectors for *EphA7* or *EfnA5* into layer 5 neurons in the frontal area or parietal area of the cortex to suppress these molecules preferentially in the corticospinal neurons (Figs. 5*A*, 9*A*,*B*). Upon KD of *EphA7* in the frontal cortex, we observed that collaterals became longer compared with control (sh*Scramble*: CEI, 0.77 ± 0.01; $n = 6$ mice; sh*EphA7-#5*: CEI, 0.90 ± 0.01; $n = 5$ mice; Welch's *t* test, $p < 0.0001$; Fig. 9*C*,*D*). Consistent with the results of DiI tracing in *EphA7*$^{-/-}$ mice (Fig. 7*D*), these data suggest that EphA7 inhibits the extension of collaterals into the BP. Interestingly, we found that KD of *EfnA5* in the parietal cortex also resulted in longer axon collaterals (sh*Scramble*: CEI, 0.77 ± 0.004; $n = 6$ mice; sh*EfnA5-#5*: CEI, 0.91 ± 0.004; $n = 6$ mice; Welch's *t* test, $p < 0.0001$; Fig. 9*C*,*E*), suggesting that

EfnA5 reverse signaling also inhibits the extension of collaterals into the BP. We next investigated whether the expression of these molecules in the cortex is involved in the regulation of the projection area of axon collaterals in the BP. We found that *EfnA5* KD in the parietal cortex resulted in a rich collateral extension in the rostral BP where *EphA7* was expressed [sh*Scramble* ($n = 6$ mice) vs sh*EfnA5-#5* ($n = 6$ mice), Welch's t test; bin 1: $0.9 \pm 0.3\%$ vs $6.7 \pm 0.8\%$, $p = 0.0005$; bin 2: $1.4 \pm 0.4\%$ vs $9.8 \pm 3.0\%$, $p = 0.037$; bin 3: $2.8 \pm 1.2\%$ vs $13.2 \pm 3.8\%$, $p = 0.038$; bin 4: $6.2 \pm 2.3\%$ vs $16.8 \pm 2.6\%$, $p = 0.00997$; bin 8: $20.1 \pm 0.9\%$ vs $9.2 \pm 2.5\%$, $p = 0.0052$; bin 9: $13.9 \pm 2.3\%$ vs $2.3 \pm 0.4\%$, $p = 0.004$; Figs. 1*C*, 2, 9*E*,*G*], whereas *EphA7* KD in the frontal cortex resulted in an abundant extension of projections in the caudal BP where *EfnA5* was expressed [sh*Scramble* ($n = 6$ mice) vs sh*EphA7-#5* ($n = 5$ mice), Welch's t test; bin 3: $5.0 \pm 0.7\%$ vs $1.9 \pm 0.7\%$, $p = 0.011$; bin 4: $13.9 \pm 1.3\%$ vs $3.3 \pm 0.5\%$, $p = 0.0002$; bin 5: $26.1 \pm 1.2\%$ vs $9.7 \pm 0.6\%$, $p < 0.0001$; bin 8: $11.0 \pm 1.1\%$ vs $19.9 \pm 1.2\%$, $p = 0.0004$; bin 9: $3.5 \pm 0.8\%$ vs $17.9 \pm 1.1\%$, $p < 0.0001$; bin 10: $1.2 \pm 0.3\%$ vs $9.5 \pm 1.2\%$, $p = 0.002$; Figs. 1*C*, 2, 9*D*,*F*]. We next overexpressed EphA7 in layer 5 neurons of a broad region of cortex (including frontal and parietal areas) and found abundant collaterals around the center bins [control ($n = 4$ mice) vs EphA7 ($n = 3$ mice), Dunnett's test; bin 4: $13.0 \pm 1.7\%$ vs $26.2 \pm 1.6\%$, $p < 0.0001$; bin 5: $18.7 \pm 2.7\%$ vs $25.2 \pm 0.4\%$, $p = 0.037$; bin 7: $18.7 \pm 0.9\%$ vs $10.8 \pm 1.3\%$, $p = 0.0005$; bin 8: $11.2 \pm 1.3\%$ vs $2.7 \pm 0.6\%$, $p = 0.0093$; Figs. 1*C*, 2, 10*A*–*C*], whereas ectopically expressed EfnA5 in layer 5 neurons of a broad region of the cortex (including the frontal and parietal areas) resulted in the abundant caudally biased collateral extension [control ($n = 4$ mice) vs EfnA5 ($n = 6$ mice), Dunnett's test; bin 4: $13.0 \pm 1.7\%$ vs $5.3 \pm 0.4\%$, $p = 0.0008$; bin 5: $18.7 \pm 2.7\%$ vs $7.4 \pm 0.5\%$, $p = 0.0004$; bin 6: $18.2 \pm 1.8\%$ vs $8.9 \pm 0.7\%$, $p = 0.0002$; bin 7: $18.7 \pm 0.9\%$ vs $8.9 \pm 0.7\%$, $p < 0.0001$; bin 9: $5.4 \pm 2.3\%$ vs $25.6 \pm 1.9\%$, $p < 0.0001$; bin 10: $2.8 \pm 0.7\%$ vs $16.6 \pm 1.6\%$, $p < 0.0001$; Figs. 1*C*, 2, 10*A*–*C*].

Finally, we had EfnA5 or EphA7 exogenously expressed in the BP to study how each gene impacts regional organization of the corticopontine projection. To this end, we electroporated EfnA5- or

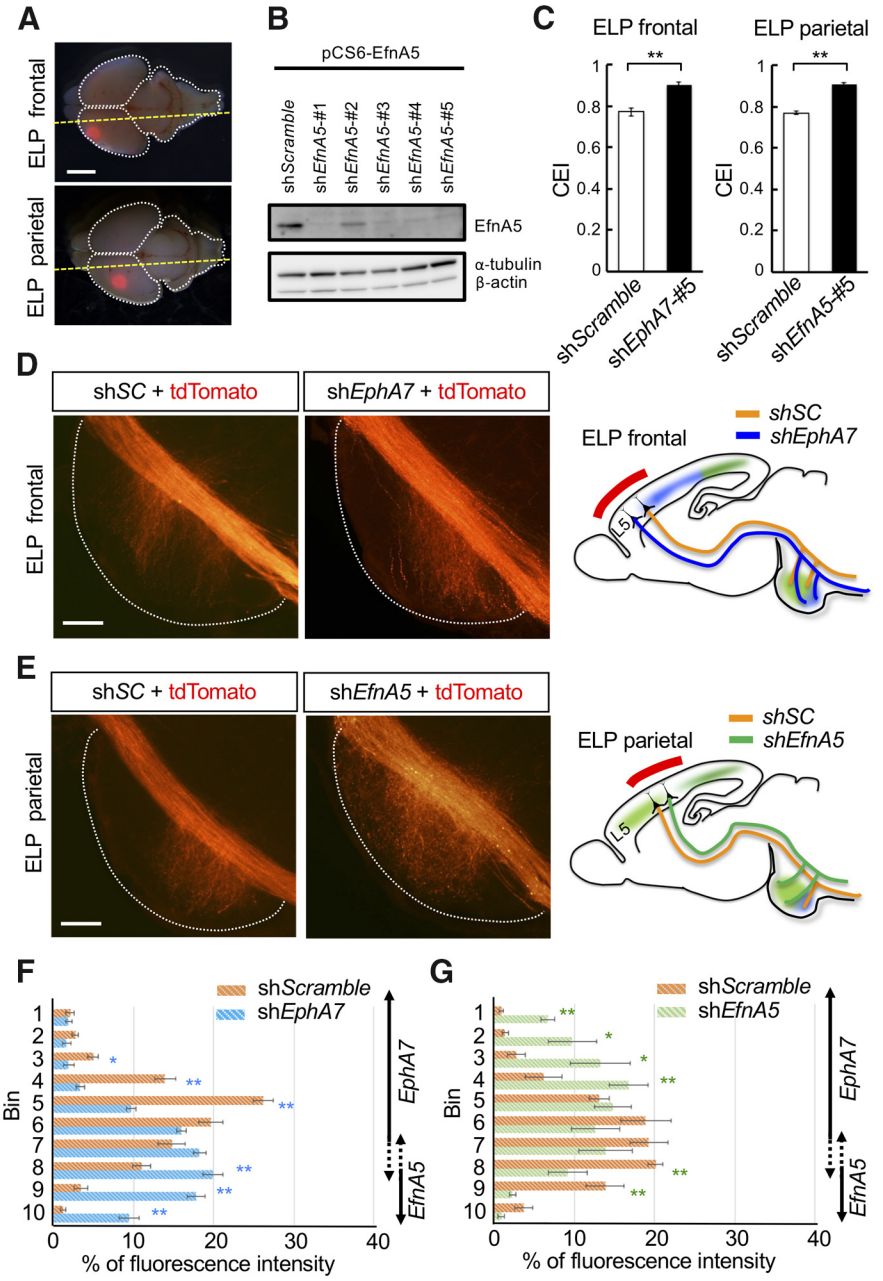

Figure 9. Projection area of the axon collaterals are controlled by EphA7 forward signaling and EfnA5 reverse signaling in the corticospinal axons. ***A***, A KD plasmid for *EphA7* or *EfnA5* together with tdTomato expression vector was transfected into layer 5 corticospinal neurons by *in utero* electroporation (ELP) at E12.5 and expressed in the frontal or parietal area of the cortex. Brains were collected at P2. The cutting plane for observation is shown as a yellow dotted line. Scale bar, 2 mm. ***B***, KD efficiency of *EfnA5*-KD vectors was evaluated by immunoblotting using the HEK293T cell lysate, which expressed EfnA5 together with shRNA vectors. sh*EfnA5-#5* was used for *in vivo* KD experiments because of the highest KD efficiency. Tubulin and actin were loading controls. ***C***, CEI was calculated. KD of *EphA7* in the corticospinal neurons of frontal area and KD of *EfnA5* in the corticospinal neurons of parietal area resulted in elongated axon collaterals. Values are the mean ± SEM. Welch's t test, $^{**}p < 0.01$. ELP frontal: sh*Scramble*, $n = 6$; sh*EphA7-#5*, $n = 5$; ELP parietal: sh*Scramble*, $n = 6$; sh*EfnA5-#5*, $n = 6$. ***D–G***, Distribution of axonal collaterals along the rostrocaudal axis of the BP was estimated as fluorescence intensity in each bin. ***D***, ***E***, Representative images and summary of results are shown. KD of *EphA7* in the corticospinal neurons of frontal area (***D***, ***F***) or KD of *EfnA5* in the corticospinal neurons of parietal area (***E***, ***G***) resulted in longer and distorted axon collaterals. Axon collaterals invaded the pontine subregions where the repulsive binding partner was localized. Regions of EphA7 and EfnA5 expression corresponding to each bin were shown on the right side of the graph (***F***, ***G***). See also Figure 1*C*. Values are the mean ± SEM. Welch's t test: $^{*}p < 0.05$, $^{**}p < 0.01$. ELP frontal: sh*Scramble*, $n = 6$; sh*EphA7*, $n = 5$; ELP parietal: sh*Scramble*, $n = 6$; sh*EfnA5*, $n = 6$. Scale bars, 100 µm. sh*SC*, sh*Scramble*.

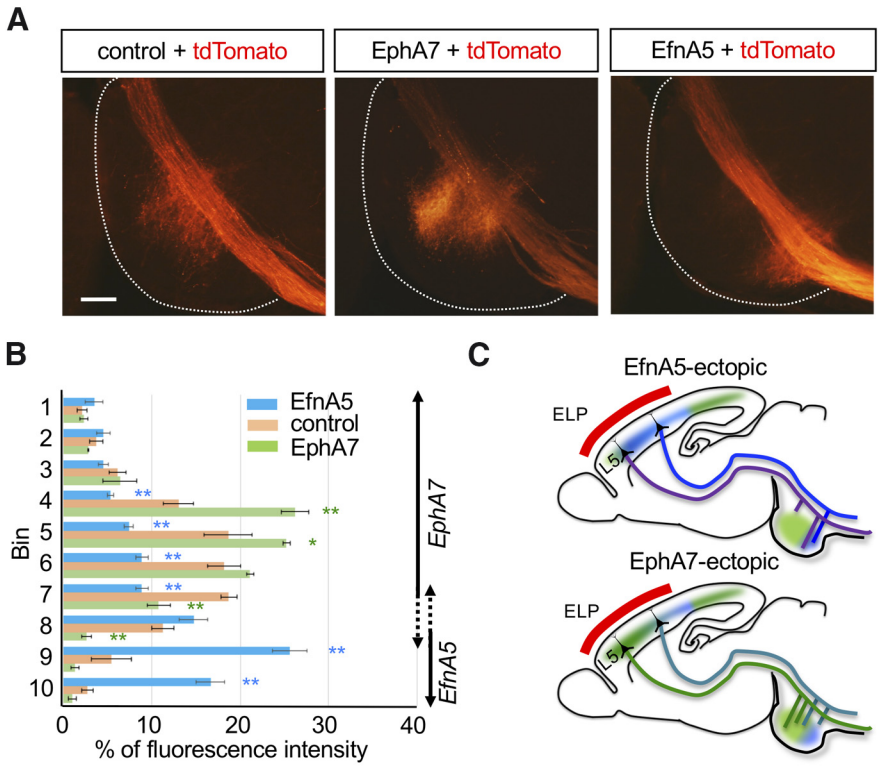

Figure 10. Ectopic expression of EphA7 and EfnA5 in the corticospinal axons limits the projection area of the axon collaterals in the BP to the region where each molecule is expressed. ***A***, ***B***, EphA7 or EfnA5 expression plasmids were transfected into the cortical neurons. When EphA7 was overexpressed in the broad area of the cortex, abundant collaterals were formed around the center region of the BP. When EfnA5 was overexpressed in the cerebral cortex, axon collaterals were formed mostly in the caudal region of the BP. ***B***, Regions of EphA7 and EfnA5 expression corresponding to each bin were shown on the right side of the graph. See also Figure 1*C*. ***C***, Summary of the results. Values are the mean ± SEM. Dunnett's test: $^{*}p < 0.05$, $^{**}p < 0.01$. Control, $n = 4$; EphA7, $n = 3$; EfnA5, $n = 6$. Scale bar, 100 µm.

EphA7-expressing vectors into the rhombic lip, where future pontine nucleus neurons are generated (Fig. 11*A*). Since the pontine nucleus neurons comprise three subpopulations derived from different progenitor subsets in the rhombic lip (Kratochwil et al., 2017), it is feasible to transfect genes of interest in the rostral, middle, or caudal region of the BP. When we electroporated EfnA5-expressing vectors and injected DiI into the frontal cortex, we found that pontine neurons with ectopic expression of EfnA5 were only localized in the middle and caudal regions of the BP, and that DiI traced frontal areal cortical neurons only extended their collaterals toward the rostral part [control ($n = 4$ mice) vs EfnA5 ($n = 3$ mice), Welch's t test; bin 1: 2.0 ± 0.8% vs 6.8 ± 1.1%, $p = 0.026$; bin 2: 2.1 ± 0.7% vs 5.6 ± 0.7%, $p = 0.015$; bin 8: 23.4 ± 1.3% vs 6.5 ± 0.7%, $p = 0.00{,}019$; bin 9: 14.8 ± 1.0% vs 5.9 ± 1.5%, $p = 0.0099$; Fig. 11*B*,*C*]. Interestingly, the frontal areal cortical neurons did not extend their collaterals into the intrapontine boundary of *EphA7* and *EfnA5* in mice with exogenous EfnA5 in the BP. In contrast, when we ectopically expressed EphA7 in the middle and caudal regions of the BP and injected DiI into the parietal cortex, DiI-traced parietal areal neurons extended their collaterals to the most caudally restricted region of the BP [control ($n = 3$ mice) vs EphA7 ($n = 3$ mice), Welch's t test; bin 8: 20.5 ± 2.9% vs 9.0 ± 2.8%, $p = 0.044$; bin 10: 9.2 ± 0.8% vs 29.8 ± 3.9%, $p = 0.03$; Fig. 11*D*,*E*].

Together, our cumulative data put forward a model in which forward and reverse signaling by receptor tyrosine kinase EphA7 and its repulsive binding partner EfnA5 coordinate restricted projection patterns from the cortex to the BP. In this manner, by regulated collateral extension, cortical and subcortical areas establish regionally segregated neural circuits during brain development.

Discussion

In this work, we discovered that collateral extension is regulated by the mutually repulsive molecules EphA7 and EfnA5. Although the complementary expression patterns of EphA7 and EfnA5 in the adult hints at a developmental mechanism that might underlie the creation of functionally distinct regions, there has been no demonstration of an inhibitory mechanism for the corticopontine collateral extension to date. Since numerous studies demonstrate the significance of pons-derived chemoattraction for the establishment of corticopontine projections (Heffner et al., 1990; Sato et al., 1994), the contribution of inhibitory mechanisms was an unexpected finding.

Developing cortical functional areas are segregated from each other through mutual repulsion between EphA7 and EfnA5. Similarly, EphA7-positive collaterals avoid EfnA5-positive pontine regions, and EfnA5-positive collaterals avoid EphA7-positive pontine regions. The stripe assays with RCFS cortical slices, which we established here, clearly showed areal preference of cortical axons for EfnA5, and growth cone collapse assays indicated that EphA7 is the major receptor for EfnA5 in corticospinal neurons. Because extending collaterals interact with the dendrites of pontine neurons in the BP (Bastmeyer et al., 1998) and the dendritic morphology could be regulated by EphA7 signaling (Clifford et al., 2014), it is likely that pontine neuronal dendrites as well as the cell body play a crucial role for EphA7–EfnA5 interactions. In addition, since dendrites of the pontine neurons fill the pontine nucleus, it is likely that such collateral–dendrite interaction hinders unnecessarily widespread and/or extended collateral formation, yet the involvement of diffusible repulsive cues are not fully excluded.

It is reasonable to ask why axons of the main shaft of corticospinal tract do not respond to regionally expressed EphA7 and EfnA5 in the pontine nuclei despite their responsiveness, as revealed by our stripe assay. Moreover, primary axons pass through the pontine nuclei, whereas the axon collaterals would be in the immediate vicinity of inhibitory activity of EphA7–EfnA5. We surmise that EphA7 and EfnA5 are not expressed at sufficiently high levels or that the dendrites of the pontine neurons are not sufficiently developed at the developmental time point when primary axons pass. AP binding images showed high binding activity of EfnA5 on the internal capsule and the cerebral peduncle, but low binding activity on the corticospinal main shaft near the BP in the P2 brain. Therefore, the transport of EphA7 to the axonal growth cone might not be enough to react when the main shaft passes through the pontine nucleus.

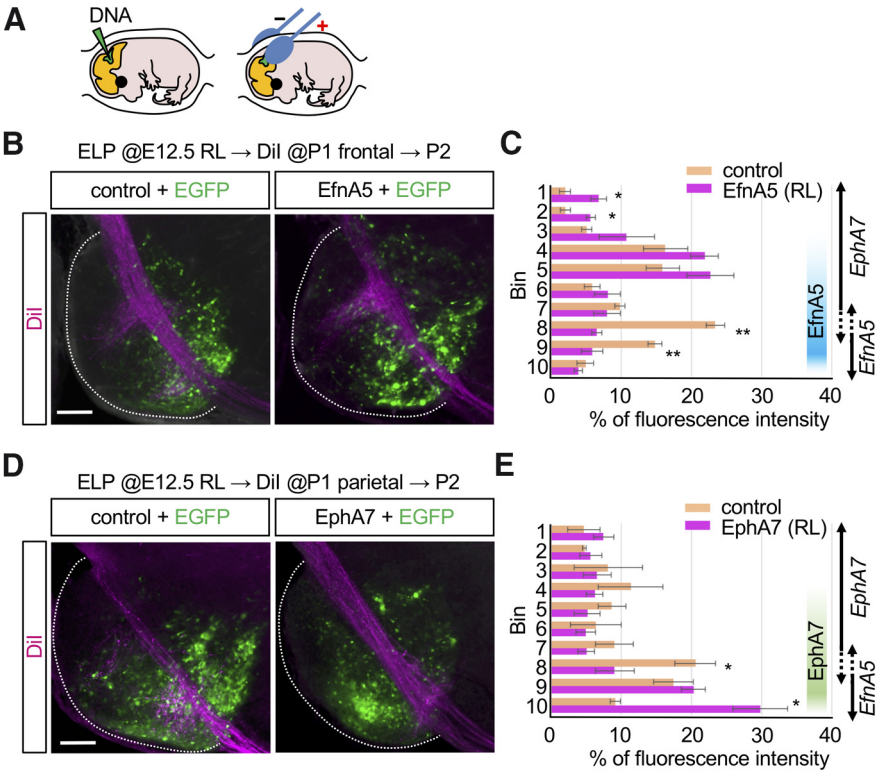

Figure 11. EphA7 forward signaling and EfnA5 reverse signaling from the pontine nuclei control the projection area of the axon collaterals of corticospinal axons. ***A***, Experimental procedures for introducing expression vectors into the pontine nuclei by *in utero* electroporation in the rhombic lip (RL). ***B***, EfnA5 expression plasmid and EGFP expression plasmid were transfected into the future pontine neurons at E12.5, so that exogenous EfnA5 was expressed in the caudal half of the BP. DiI tracer was injected into the corticospinal tract neurons in the frontal area of the cerebral cortex at P1, and the BP was observed at P2. ***C***, Distribution of axonal collaterals along the rostrocaudal axis of the BP was estimated according to fluorescence intensity in each bin. Values are the mean ± SEM. Welch's *t* test: $*p < 0.05$, $**p < 0.01$. Control, $n = 4$; EfnA5, $n = 3$. Scale bar, 100 µm. ***D***, EphA7 expression plasmid and EGFP expression plasmid were transfected into the future pontine neurons as explained in ***B***. DiI tracer was injected into the corticospinal tract neurons in the parietal area of the cerebral cortex at P1, and the BP was observed at P2. ***E***, Distribution of axonal collaterals in each bin. Values are the mean ± SEM. Welch's *t* test: $*p < 0.05$. Control, $n = 3$; EphA7, $n = 3$. Scale bar, 100 µm.

However, we cannot exclude the possibility that desensitizing mechanisms against EphA7 and/or EfnA5 exist in the primary axon tips since the extension of primary axons slows down as they pass through the pons, which results in a "waiting period" (Szebenyi et al., 1998; Canty and Murphy, 2008).

While axon collaterals with *EphA7*$^{-/-}$, or with KD of either *EphA7* or *EfnA5*, elongated longer in the BP compared with control, their phenotypes were not identical. Whereas axon collaterals of the *EphA7*$^{-/-}$ corticospinal neuron of frontal cortex extended in a manner similar to those in WT in their rostrocaudal axis, those of *EphA7* KD frontal neurons entered the caudal region of the pontine nuclei, where *EfnA5* is localized. On the other hand, axon collaterals of both *EphA7*$^{-/-}$ and *EfnA5* KD parietal neurons entered the rostral region of the pontine nuclei where *EphA7* is localized. Moreover, axon collaterals of *EfnA5* KD parietal neurons entered the most rostral regions of the BP, where those of *EphA7*$^{-/-}$ did not enter. Such a difference made us reaffirm the importance of expression patterns of EphA7 and EfnA5 both in the cerebral cortex and the BP for the region-to-region connections between them. There might be a compensation mechanism for EphA7 function in *EphA7*$^{-/-}$, because the acute insufficiency of EphA7 due to shRNA resulted in more severe phenotypes of the distribution of axon collaterals than the *EphA7*$^{-/-}$ mice. Moreover, the fact that axon collaterals were attracted toward the BP even in the absence of EphA7–EfnA5 signaling made us rerecognize the chemotropic activity of the BP. We showed here that EphA7-mediated forward signaling and EfnA5-mediated reverse signaling between cortical neurons and pontine neurons are necessary for region-to-region connections. However, it remains possible that other Eph–Efn signals and/or effects of *cis* interaction of Eph and Efn (Fiederling et al., 2017) also make contributions to shaping the precise formation of corticopontine projections.

In the caudomedial region of the BP, projections from the frontal cortex and the parietal cortex do not show an obvious boundary (Leergaard and Bjaalie, 2007). The caudomedial region of the BP is the region where layer 5 cortical neurons, in the vicinity of the boundary of *EphA7*-positive and *EfnA5*-positive areas, extend their axon collaterals. Our data suggest that this is likely because different expression levels of *EphA7* in the neocortex will result in a different degree of response to *EfnA5*. According to our *in situ* hybridization data, layer 5 neurons in the occipital cortical area expressed high levels of *EphA7* with a sharp boundary to the *EfnA5*-expressing parietal area, whereas layer 5 neurons in the frontal cortex expressed low levels of *EphA7*, forming an ambiguous boundary with the *EfnA5*-expressing parietal cortex. Moreover, when we overexpressed EphA7 in the frontal cortex, we observed that collateral extension was more limited, with less extension in the caudomedial region of the BP (Fig. 10). The fact that the frontal areal cortical neurons did not extend their collaterals over the intrapontine boundary of *EphA7* and *EfnA5* in mice with exogenous EfnA5 in the caudal half of the BP (Fig. 11*B*,*C*) also supports this notion. Interestingly, it should be noted that motor cortex and somatosensory cortex are not so sharply divided, and in fact overlap to some extent in rodents compared with primates (Ragsdale and Grove, 2001).

What upstream mechanism controls the regional specificity of EphA7 and EfnA5 is an interesting question to investigate. The pontine nucleus comprises three different progenitor origins generated in the rhombic lip, which are distinguished by combinations of *Hox* genes expressed (Di Meglio et al., 2013; Kratochwil et al., 2017). Different expression of *Hox* family genes is known to regulate segmentation of the rhombomere by controlling the expression of Eph receptors (Prin et al., 2014). Recently, Hox5-dependent positional identity of rostral pontine neurons and connectivity of somatosensory cortical afferents to the BP are shown (Maheshwari et al., 2020). We showed ectopic expression of *EfnA5* in the rostral region of the BP in *EphA7*$^{-/-}$. It is possible that *EfnA5*-expressing cells have invaded the region

originally occupied by *EphA7*-expressing cells during migration from the rhombic lip to the BP. Thus, it is possible that *Hox* genes create a protomap of region-to-region connections by controlling the expression pattern of EphA7 and EfnA5 in the BP.

The pontine nuclei functions as a relay between cerebral cortex and the cerebellum, and, interestingly, there is also a regionally organized circuit connection between the pontine nuclei and the cerebellum (Odeh et al., 2005). Given that EphA7 and EfnA5 exhibits region-specific exclusive expression in the cerebellum (Rogers et al., 1999), it could well be that the EphA7–EfnA5 axis plays a crucial role in the pontine nuclei to cerebellum projection as well. Therefore, the EphA7–EfnA5 axis may provide a framework for region-to-region connections of the cortico-ponto-cerebellar pathway. Moreover, since EphA7–EfnA5 is expressed in a mutually exclusive manner in subregions of other targets of subcortical projections, such as the superior colliculus (Rashid et al., 2005) and inferior olivary nucleus (Nishida et al., 2002), this axis seems poised to provide a common molecular framework for regional segregation of information from different cortical areas throughout the corticospinal tract and related brain regions.

References

Arai Y, Pierani A (2014) Development and evolution of cortical fields. Neurosci Res 86:66–76.

Bastmeyer M, Daston MM, Possel H, O'Leary DDM (1998) Collateral branch formation related to cellular structures in the axon tract during corticopontine target recognition. J Comp Neurol 392:1–18.

Brissenden JA, Tobyne SM, Osher DE, Levin EJ, Halko MA, Somers DC (2018) Topographic cortico-cerebellar networks revealed by visual attention and working memory. Curr Biol 28:3364–3372.e5.

Brodal P, Bjaalie JG (1992) Organization of the pontine nuclei. Neurosci Res 13:83–118.

Cang J, Kaneko M, Yamada J, Woods G, Stryker MP, Feldheim DA (2005) Ephrin-As guide the formation of functional maps in the visual cortex. Neuron 48:577–589.

Canty AJ, Murphy M (2008) Molecular mechanisms of axon guidance in the developing corticospinal tract. Prog Neurobiol 85:214–235.

Clifford MA, Athar W, Leonard CE, Russo A, Sampognaro PJ, Van der Goes MS, Burton DA, Zhao X, Lalchandani RR, Sahin M, Vicini S, Donoghue MJ (2014) EphA7 signaling guides cortical dendritic development and spine maturation. Proc Natl Acad Sci U S A 111:4994–4999.

Cong L, Ran FA, Cox D, Lin S, Barretto R, Habib N, Hsu PD, Wu X, Jiang W, Marraffini LA, Zhang F (2013) Multiplex genome engineering using CRISPR/Cas systems. Science 339:819–823.

Di Meglio T, Kratochwil CF, Vilain N, Loche A, Vitobello A, Yonehara K, Hrycaj SM, Roska B, Peters AHFM, Eichmann A, Wellik D, Ducret S, Rijli FM (2013) *Ezh2* orchestrates topographic migration and connectivity of mouse precerebellar neurons. Science 339:204–207.

Egea J, Klein R (2007) Bidirectional Eph–ephrin signaling during axon guidance. Trends Cell Biol 17:230–238.

Fiederling F, Weschenfelder M, Fritz M, Von Philipsborn A, Bastmeyer M, Weth F (2017) Ephrin-A/EphA specific co-adaptation as a novel mechanism in topographic axon guidance. Elife 6:e25533.

Flanagan JG, Leder P (1990) The kit ligand: a cell surface molecule altered in steel mutant fibroblasts. Cell 63:185–194.

Gao Z, Davis C, Thomas AM, Economo MN, Abrego AM, Svoboda K, De Zeeuw CI, Li N (2018) A cortico-cerebellar loop for motor planning. Nature 563:113–116.

Greig LC, Woodworth MB, Galazo MJ, Padmanabhan H, Macklis JD (2013) Molecular logic of neocortical projection neuron specification, development and diversity. Nat Rev Neurosci 14:755–769.

Heffner CD, Lumsden A, O'Leary DDM (1990) Target control of collateral extension and directional axon growth in the mammalian brain. Science 247:217–220.

Iguchi T, Yagi H, Wang C-C, Sato M (2012) A tightly controlled conditional knockdown system using the Tol2 transposon-mediated technique. PLoS One 7:e33380.

Janis LS, Cassidy RM, Kromer LF (1999) Ephrin-A binding and EphA receptor expression delineate the matrix compartment of the striatum. J Neurosci 19:4962–4971.

Joshi PS, Molyneaux BJ, Feng L, Xie X, Macklis JD, Gan L (2008) Bhlhb5 regulates the postmitotic acquisition of area identities in layers II-V of the developing neocortex. Neuron 60:258–272.

Kratochwil CF, Maheshwari U, Rijli FM (2017) The long journey of pontine nuclei neurons: from rhombic lip to cortico-ponto-cerebellar circuitry. Front Neural Circuits 11:33.

Lai KO, Ip NY (2009) Synapse development and plasticity: roles of ephrin/Eph receptor signaling. Curr Opin Neurobiol 19:275–283.

Leergaard TB, Bjaalie JG (2007) Topography of the complete corticopontine projection: from experiments to principal maps. Front Neurosci 1:211–223.

Leergaard TB, Lakke EAJF, Bjaalie JG (1995) Topographical organization in the early postnatal projection: a carbocyanine dye and 3-D computer reconstruction study in the rat. J Comp Neurol 361:77–94.

Liu Z-Q (1991) Scale space approach to directional analysis of images. Appl Opt 30:1369.

Low LK, Liu X-B, Faulkner RL, Coble J, Cheng H-J (2008) Plexin signaling selectively regulates the stereotyped pruning of corticospinal axons from visual cortex. Proc Natl Acad Sci U S A 105:8136–8141.

Maheshwari U, Kraus D, Vilain N, Holwerda SJB, Cankovic V, Maiorano NA, Kohler H, Satoh D, Sigrist M, Arber S, Kratochwil CF, Di Meglio T, Ducret S, Rijli FM (2020) Postmitotic Hoxa5 expression specifies pontine neuron positional identity and input connectivity of cortical afferent subsets. Cell Rep 31:107767.

Mashiko D, Fujihara Y, Satouh Y, Miyata H, Isotani A, Ikawa M (2013) Generation of mutant mice by pronuclear injection of circular plasmid expressing Cas9 and single guided RNA. Sci Rep 3:3355.

Miller K, Kolk SM, Donoghue MJ (2006) EphA7-ephrin-A5 signaling in mouse somatosensory cortex: developmental restriction of molecular domains and postnatal maintenance of functional compartments. J Comp Neurol 496:627–642.

Nagano T, Yoneda T, Hatanaka Y, Kubota C, Murakami F, Sato M (2002) Filamin A-interacting protein (FILIP) regulates cortical cell migration out of the ventricular zone. Nat Cell Biol 4:495–501.

Niethamer TK, Bush JO (2019) Getting direction(s): the Eph/ephrin signaling system in cell positioning. Dev Biol 447:42–57.

Nishida K, Flanagan JG, Nakamoto M (2002) Domain-specific olivocerebellar projection regulated by the EphA-ephrin-A interaction. Development 129:5647–5658.

Niwa H, Yamamura K, Miyazaki J (1991) Efficient selection for high-expression transfectants with a novel eukaryotic vector. Gene 108:193–199.

Odeh F, Ackerley R, Bjaalie JG, Apps R (2005) Pontine maps linking somatosensory and cerebellar cortices are in register with climbing fiber somatotopy. J Neurosci 25:5680–5690.

O'Leary DDM, Koester SE (1993) Development of projection neuron types, axon pathways, and patterned connections of the mammalian cortex. Neuron 10:991–1006.

O'Leary DDM, Terashima T (1988) Cortical axons branch to multiple subcortical targets by interstitial axon budding: implications for target recognition and "waiting periods". Neuron 1:901–910.

O'Leary DDM, Chou S-J, Sahara S (2007) Area patterning of the mammalian cortex. Neuron 56:252–269.

Prin F, Serpente P, Itasaki N, Gould AP (2014) Hox proteins drive cell segregation and non-autonomous apical remodelling during hindbrain segmentation. Development 141:1492–1502.

Ragsdale CW, Grove EA (2001) Patterning the mammalian cerebral cortex. Curr Opin Neurobiol 11:50–58.

Ramnani N (2006) The primate cortico-cerebellar system: anatomy and function. Nat Rev Neurosci 7:511–522.

Rashid T, Upton AL, Blentic A, Ciossek T, Knöll B, Thompson ID, Drescher U (2005) Opposing gradients of Ephrin-As and EphA7 in the superior colliculus are essential for topographic mapping in the mammalian visual system. Neuron 47:57–69.

Rogers JH, Ciossek T, Menzel P, Pasquale EB (1999) Eph receptors and ephrins demarcate cerebellar lobules before and during their formation. Mech Dev 87:119–128.

Sato M, Lopez-Mascaraque L, Heffner CD, O'Leary DDM (1994) Action of a diffusible target-derived chemoattractant on cortical axon branch induction and directed growth. Neuron 13:791–803.

Sensini A, Gualandi C, Zucchelli A, Boyle LA, Kao AP, Reilly GC, Tozzi G, Cristofolini L, Focarete ML (2018) Tendon fascicle-inspired nanofibrous scaffold of polylactic acid/collagen with enhanced 3D-structure and biomechanical properties. Sci Rep 8:17167.

Serizawa S, Miyamichi K, Takeuchi H, Yamagishi Y, Suzuki M, Sakano H (2006) A neuronal identity code for the odorant receptor-specific and activity-dependent axon sorting. Cell 127:1057–1069.

Stanfield BB, O'Leary DDM, Fricks C (1982) Selective collateral elimination in early postnatal development restricts cortical distribution of rat pyramidal tract neurones. Nature 298:371–373.

Szebenyi G, Callaway JL, Dent EW, Kalil K (1998) Interstitial branches develop from active regions of the axon demarcated by the primary growth cone during pausing behaviors. J Neurosci 18:7930–7940.

Tiong SYX, Oka Y, Sasaki T, Taniguchi M, Doi M, Akiyama H, Sato M (2019) *Kcnab1* is expressed in subplate neurons with unilateral long-range inter-areal projections. Front Neuroanat 13:39.

Torii M, Levitt P (2005) Dissociation of corticothalamic and thalamocortical axon targeting by an EphA7-mediated mechanism. Neuron 48:563–575.

Wagner MJ, Luo L (2020) Neocortex–cerebellum circuits for cognitive processing. Trends Neurosci 43:42–54.

Weschenfelder M, Weth F, Knöll B, Bastmeyer M (2013) The stripe assay: studying growth preference and axon guidance on binary choice substrates in vitro. Methods Mol Biol 1018:229–246.

Yamagishi S, Kesavamoorthy G, Bastmeyer M, Sato K (2016) Stripe assay to study the attractive or repulsive activity of a protein substrate using dissociated hippocampal neurons. J Vis Exp. 112:e54096.

Zembrzycki A, Perez-Garcia CG, Wang C-F, Chou S-J, O'Leary DDM (2015) Postmitotic regulation of sensory area patterning in the mammalian neocortex by Lhx2. Proc Natl Acad Sci U S A 112:6736–6741.

Zhu Y, Matsumoto T, Mikami S, Nagasawa T, Murakami F (2009) SDF1/CXCR4 signalling regulates two distinct processes of precerebellar neuronal migration and its depletion leads to abnormal pontine nuclei formation. Development 136:1919–1928.